117
10-21-80
JWB

Dr. 1854

GA-A15974
UC-20

MASTER

THE TEAM ONE (GA/MCA) EFFORT OF THE DOE 12 TESLA COIL DEVELOPMENT PROGRAM

12 TESLA ETF TOROIDAL FIELD COIL HELIUM BATH COOLED NbTi ALLOY CONCEPT

by
PROJECT STAFF

JULY 1980

DISTRIBUTION OF THIS DOCUMENT IS UNLIMITED

GENERAL ATOMIC COMPANY

DISCLAIMER

This report was prepared as an account of work sponsored by an agency of the United States Government. Neither the United States Government nor any agency Thereof, nor any of their employees, makes any warranty, express or implied, or assumes any legal liability or responsibility for the accuracy, completeness, or usefulness of any information, apparatus, product, or process disclosed, or represents that its use would not infringe privately owned rights. Reference herein to any specific commercial product, process, or service by trade name, trademark, manufacturer, or otherwise does not necessarily constitute or imply its endorsement, recommendation, or favoring by the United States Government or any agency thereof. The views and opinions of authors expressed herein do not necessarily state or reflect those of the United States Government or any agency thereof.

DISCLAIMER

Portions of this document may be illegible in electronic image products. Images are produced from the best available original document.

DISCLAIMER

This report was prepared as an account of work sponsored by an agency of the United States Government. Neither the United States Government nor any agency thereof, nor any of their employees, makes any warranty, express or implied, or assumes any legal liability or responsibility for the accuracy, completeness, or usefulness of any information, apparatus, product, or process disclosed, or represents that its use would not infringe privately owned rights. Reference herein to any specific commercial product, process, or service by trade name, trademark, manufacturer, or otherwise, does not necessarily constitute or imply its endorsement, recommendation, or favoring by the United States Government or any agency thereof. The views and opinions of authors expressed herein do not necessarily state or reflect those of the United States Government or any agency thereof.

Printed in the United States of America
Available from
National Technical Information Service
U.S. Department of Commerce
5285 Port Royal Road
Springfield, Virginia 22161

NTIS Price Codes:
Printed copy: A05
Microfiche: A01

GA-A15974
UC-20

THE TEAM ONE (GA/MCA) EFFORT OF THE DOE 12 TESLA COIL DEVELOPMENT PROGRAM

12 TESLA ETF TOROIDAL FIELD COIL HELIUM BATH COOLED NbTi ALLOY CONCEPT

DISCLAIMER

This book was prepared as an account of work sponsored by an agency of the United States Government. Neither the United States Government nor any agency thereof, nor any of their employees, makes any warranty, express or implied, or assumes any legal liability or responsibility for the accuracy, completeness, or usefulness of any information, apparatus, product, or process disclosed, or represents that its use would not infringe privately owned rights. Reference herein to any specific commercial product, process, or service by trade name, trademark, manufacturer, or otherwise, does not necessarily constitute or imply its endorsement, recommendation, or favoring by the United States Government or any agency thereof. The views and opinions of authors expressed herein do not necessarily state or reflect those of the United States Government or any agency thereof.

by
PROJECT STAFF

Prepared under
Department of Energy
Contract DE-AT03-76ET51011

GENERAL ATOMIC PROJECT 3235
JULY 1980

DISTRIBUTION OF THIS DOCUMENT IS UNLIMITED

GENERAL ATOMIC COMPANY

THIS PAGE

WAS INTENTIONALLY

LEFT BLANK

ABSTRACT

This report presents the conceptual design of an ETF compatible toroidal field coil, employing helium bath cooled NbTi alloy conductor. It constitutes fulfillment by Team One (GA/MCA) of Phase II of its effort in the DOE/OFE/D&T 12 Tesla Coil Development Program (FTP/A No. 16869). This study provides continuity of the entire Team One effort, ensuring that the prototypical conductor as developed is reactor compatible, and establishing the viability of an actual reactor TF-coil concept employing such conductor.

The ten TF-coil array generates a peak field of 11-1/2 tesla at 2.87 m radius, corresponding to a major axis field of 6.1 tesla. The 10 kA conductor is an uninsulated, unsoldered "Rutherford" cable, employing NbTiTa alloy as developed in Phase I of this effort. The conductor is encased within a four element "frame" of stainless steel strips to provide hoop and bearing load support.

The coils are pancake wound directly onto the weldment formed by the central, radial spine, and inner perimeter wall of the stainless steel helium vessel. Overall current density of the coil/helium vessel in the annular centerpost region is 1000 amp/cm^2, for an average conductor current density of 4794 amp/cm^2.

The helium bath is pumped to 0.24 atmosphere, corresponding to a saturation temperature of 3 K. The bath is heat exchanger subcooled to an operating temperature of 2.5 K, providing an adequate margin for single phase absorbtion of a plasma disruption.

Quench protection is provided by intercoil dump resistors, voltage signal activated by mechanical switches. Verification of a coil's ability to sustain a full quench without suffering overvoltage or overtemperature damage is provided by a computer analysis, which accounts for all significant dynamic parameters.

Although not provided in the ETF Interim Design, this study indicates that the provision of diagonal inter-coil struts may be necessary to support the immense out-of-plane loads.

THIS PAGE

WAS INTENTIONALLY

LEFT BLANK

CONTENTS

FIGURES

FIGURES (Continued)

TABLES

THIS PAGE

WAS INTENTIONALLY

LEFT BLANK

X

1. INTRODUCTION

1.1. SCOPE OF WORK

This report presents the conceptual design of an ETF compatible 12 tesla toroidal field coil, employing helium bath cooled NbTi alloy conductor. It constitutes fulfillment by Team One (GA/MCA) of Phase II of its effort in the DOE/OFE/D&T 12 Tesla Coil Development Program (FTP/A No. 16869).

1.2. PARTICIPANTS

This study has been performed by General Atomic's Superconducting Magnet Group, a branch of the Fusion Division's D&T program; and by the Magnetic Corporation of America, working under subcontract to GA. Related preliminary work (Phase I) was performed during FY'79 by Dr. David Larbelestier, *et al.*, at the University of Wisconsin.

The following GA personnel participated in the study, in the capacities indicated:

Dr. Sibley Burnett	—	Fusion D&T Program Manager
John Purcell	—	Fusion D&T Program: Technical Manager
John Alcorn	—	Superconducting Magnet Group: Manager
Dr. Wilkie Chen	—	Magnetics, Stability, A-C Loss Analysis
Dr. Yen-Hwa Hsu	—	Cryogenic, Quench Analysis
Lew Creedon	—	Structural Analysis

The following MCA personnel participated in the study:

Dr. Z. J. J. Stekly
Harvey R. Segal
Ted DeWinter

1.3. TEAM ONE EFFORT OF THE DOE/OFE/D&T 12 TESLA COIL DEVELOPMENT PROGRAM

1.3.1. Mission

The basic mission of this effort is to demonstrate the feasibility of, and establish an engineering data base for utilizing helium bath cooled NbTi alloy to generate a peak toroidal field of 12 tesla in a tokamak reactor. (The other teams of this program utilize Nb_3Sn for their designs.)

General Atomic Company is the leader for Team One, with the Magnetic Corporation of America (MCA) as industrial subcontractor.

1.3.2. Scope

The four-year effort is being implemented in four closely related phases:

I. Experimental development of a NbTi alloy, compositionally and process optimized for 12 tesla operation at bath temperatures below 4 K.

II. Conceptual design of an ETF reactor compatible toroidal field coil system, employing the NbTi alloy selected by Phase I, and an appropriate bath cooling regime.

III. Design, construction and testing of a solenoid coil utilizing the selected reactor prototypical conductor and bath conditions. This coil will be tested at the LLNL High Field Test Facility.

IV. Tests performed at the GA High Field Test Facility to assist in design of the test coil and to aid interpretation of results therefrom.

Phase I was completed during FY'79 by the University of Wisconsin (Dr. David Larbelestier, *et al.*) and MCA. A ternary alloy containing 25 weight percent tantalum was selected on the basis of its upper critical field (H_{c_2}) and current density performance at temperatures in the 1.8 — 3 K range.

1.4. RELATION TO OTHER PHASES OF THE TEAM ONE EFFORT

1.4.1. General

This study of a 12 tesla ETF coil provides continuity of the entire Team One 12 tesla effort, ensuring that the prototypical conductor as developed is reactor compatible, and establishing the viability of an actual reactor TF-coil employing such conductor.

1.4.2. Relation to Phase I

(Experimental development of a NbTi alloy, compositionally and process optimized for 12 tesla operation at bath temperatures below 4 K.)

During FY 1979 the Engineering Experiment Station of the University of Wisconsin (Dr. David Larbalestier, *et al.*,) experimentally investigated the upper critical field of various NbTi alloys, as a function of chemical composition and temperature (between 4 K and 1.7 K). A ternary NbTiTa alloy (32/43/25 weight percent) was selected, which exhibits an upper critical field of 15.4 tesla at 2 K — a full tesla higher than comparable binary NbTi alloys.

MCA verified the practicality of this alloy from the standpoints of conductor processing and current density. Therefore this TF-coil design concept, and the Phase III Test Coil are based upon this material.

1.4.3. Relation to Phase III

(Design, construction and testing of a solenoid coil utilizing the selected reactor prototypical conductor and bath conditions. This coil will be tested at the LLNL High Field Test Facility.)

For a cabled conductor/support strip configuration as specified for this TF-coil design, the product of effective heat transfer rate $Q(W/cm^2)$ and effective cooled perimeter C.P. (cm) can only be determined with

confidence by superconducting recovery tests performed using similar configurations and comparable operating parameters. This data is one of the primary goals of the experiments to be performed upon the Team One Test Coil at the LLNL High Field Test Facility during FY'82.

1.4.4. Relation to Phase IV

(Tests performed at the GA High Field Test Facility to assist in design of the test coil and to aid interpretation of results therefrom.)

A test facility has been established at GA having the capability of generating 10 tesla within the 20 cm bore of its nested solenoid pair. Both background field coils employ NbTi; the 40 cm bore 8 tesla coil, built by MCA, is intrinsically stable, and without internal cooling; the insert coil was "dry" wound by GA using "barber pole" wrapped cable, supported by stainless steel strip wound on its O.D: A vacuum insulated tube can be inserted within the 20 cm bore for testing samples at subatmospheric pressure, and temperatures down to 1.8 K.

With this apparatus, heat pulse/recovery data is being obtained on various cable samples which will augment, and greatly assist interpretation of the FY'82 LLNL HFTF results. Also a series of saturated superfluid helium tests are being performed to better understand the parameters of this bath cooling option.

1.5. BASIC PARAMETERS

The basic parameters of the Team One TF-coil design concept are presented in Table 1-1.

As discussed further in Section 2, the ETF guideline parameters as regards size, number of coils, etc., are those which prevailed at the ETF Design Center in June 1980.

TABLE 1-1
ETF 12 TESLA TOROIDAL FIELD COILS — TEAM ONE CONCEPT
BASIC PARAMETERS

Number of coils	10
Total ampere turns	165×10^6
Total stored energy	40 GJ
Total inductance	800 H
Peak field	11-1/2 T
Current	10 kA
Total weight (10 coil/He vessels)	3.42×10^6 kg
Coil straight section height	7.2 m
Mean radius of outer coil leg	11.5 m
Conductor:	
Superconductor	NbTiTa
Stabilizer	Copper
Configuration	Unsoldered, 3-level Rutherford cable
Coil cooling	ℓHe bath, 3 K saturation temperature subcooled to 2.5 K
Structural material	Austenitic stainless steel

THIS PAGE

WAS INTENTIONALLY

LEFT BLANK

2. DESIGN CRITERIA

2.1. RELATION TO ETF

The magnet system presented is generic in concept for a large tokamak fusion device, such as the Engineering Test Facility (ETF). It should be pointed out that ever since establishment of the ETF Design Center in 1978, the reactor concept, and hence TF-coil requirements, have undergone continual evolution. Thus, for this and other 12 Tesla Program TF-Coil studies, it was necessary to select a set of guideline parameters at some point, and complete the design on that basis. In the case of the Team One concept, the guidelines were adjusted in mid-1980 to reflect the ETF "Design 1" parameters as regards number (10) and size of TF coils (Refs. 2-1, 2-2). Also, the peak field was reduced to 11-1/2 tesla, for reasons discussed in Subsection 2.3 below. The 10 kA current was selected primarily upon the basis of compatibility with the conductor to be used in the 12 tesla test coil of this program.

In order to identify the origins of the various requirements and constraints to which the toroidal field coils have been designed, they are presented under three generic headings: Imposed Dimensional Constraints, Functional Requirements, and Functional Burdens.

2.2. DIMENSIONAL CONSTRAINTS

These are set by physics machine size requirements, and spatial demands for other reactor components within and around the toroidal field coil envelope. The coil outer radius in the centerpost region is set by the plasma chamber dimensions and requisite inboard blanket and shield thickness (the shield requirement being set largely by the maximum allowable lifetime neutron fluence to the coil conducting and insulating components). This sets the peak field and ampere turn requirement. The outer leg mean

equatorial radius is set by internal and intercoil space demands versus the need to minimize external equilibrium (EF) coil to plasma distances (and hence currents).

The corresponding number of coils, 10, was selected by the ETF Design Center based upon maximum allowable field ripple and intercoil access considerations.

The basic dimensional constraints employed in this design are:

- Number of TF-coils 10
- Centerpost outer radius of TF-coil helium vessel 2.94 m
- Mean radius of TF-coil outer leg at equator 11.5 m

2.3. PERFORMANCE REQUIREMENTS

- Peak Toroidal Field: The peak field requirement is set by the need for a given field at the plasma axis and the maximum permissible radius of the coil in the centerpost region, as described above. In this case it was initially set simply by the program mandate for 12 tesla.

  However, the design shown herein is based upon 11-1/2 tesla peak, since it now appears that ETF will not require more than this. Reference Designs 1 and 2 of the Design Center specify 5.5 tesla at the major axis of 5.4 m, and a corresponding peak toroidal field of 11.4 T.

  As a matter of fact, the maximum TF-coil centerpost helium vessel radius of this design is 2.94 m. Allowing 6 cm for vessel wall thickness, and 1 cm for ground insulation, the peak field required is only 10.4 tesla. The additional 1 tesla results from the fact that the ETF TF-coil design employs a rectangular centerpost coil pack. Nevertheless, an additional tesla may eventually be required for various reasons, including a margin for long burn impurity control.

- Maximum Allowable Field Ripple at Plasma: The calculated peak value for a 10 coil array of the indicated imposed dimensions is ± 1.0%, which is compatible with physics requirements. The corresponding ripple at the plasma axis is ± 0.10%.

- Coils Must Accommodate Plasma Neutron Heat Flux and Normal Operational ac Heat Loads Without Jeopardizing Stability: The lifetime fluence shielding requirements for the TF-coil centerpost region materials (copper, insulation) result in a modest heat flux (5 kW) in this design.

- Coils Must Absorb Plasma Disruption Without Going Normal: This is a significant concern due to the external location of the EF-coil system.

- Coils Must be Cryogenically Stabilized Against a "Maximum Credible" Normal Operating Disturbance: The only such disturbance is local transient mechanical motion of a conductor in response to the magnetic field loads.

- Coils Must Survive All Perceived Credible Fault Conditions Without Damage: The only two major such conditions envisioned are a coil quench, initiated by low liquid level, and a sudden loss of system vacuum.

- Coils Must Meet All Above Requirements Following Exposure to the Design Lifetime Neutron Plasma Fluence.

- Coils Must Meet the Above Requirements Without Replacement of Major Components Throughout the Design Reactor Lifetime.

- TF-Coil System Must Survive All Perceived Credible Accident Conditions Without Endangering Personnel or Causing Major Damage to Other Reactor Components: This requirement includes such mishaps as a severed coil circuit, resulting in arcing and unequal coil currents.

2.4. FUNCTIONAL BURDENS

These are the quantified environmental conditions within which the TF-coils must function.

- Centerpost plasma neutron flux: 5 kW
- Plasma pulse duration: 100 sec
- Cycle duration: 135 sec
- Total lifetime fluence (max): 1×10^9 rad; equivalent to a fast neutron fluence of 1×10^{18} n/cm^2.
- Out-of-plane (overturning) moment per coil: (see Section 3, Fig. 3-3).
- Operating poloidal field experienced: $\dot{B}_\perp$ and $\dot{B}_\parallel$ = 0.15 tesla/sec for 1 sec.
- Plasma disruption field experienced: ΔB = 0.5 tesla in 500 ms.
- Conductor stability criterion: 100 mJ/cm^3 over 1 meter (GA selected).
- Peak design dump voltage: 1 kV (GA selected).

REFERENCES

2-1. "ETF Parameters," ETF-M-80-DC-057, Issue No. 4, June 25, 1980.

2-2. "ETF Interim Design Description Document," ETF Design Center, Section 5, Magnetic System Design Summary, July 1980.

3. DESIGN CONSIDERATIONS

3.1. INTRODUCTION

Basically, all of the TF-coil design considerations fall into five closely interrelated generic categories: Performance, Reliability, Reactor Compatibility, Cost, and Safety. All of these factors underlie the basic design considerations discussed below, and the resultant selected design features.

The principal specific issues confronted in design of the ETF toroidal field coils are the following:

- Selection of appropriate superconductor material.
- Coil cooling method.
- Selection of an appropriate conductor/support configuration.
- Accommodation of the eddy current heat loads induced in the coil/helium vessel structure by a plasma disruption.
- Support of the coils against the immense out-of-plane (overturning) loads generated by interaction of their current with the fringing field of the externally located equilibrium field (EF) coils.
- Verification of a coil's ability to sustain a low liquid level induced quench without damage, based upon a selected protection scheme.
- TF-coil and reactor costs.
- Reliability.
- Maintainability.
- Safety/failure modes.

3.2. SUPERCONDUCTOR/TEMPERATURE SELECTION

3.2.1. Introduction

Ten tesla is about the upper practical limit for employment of NbTi alloys cooled with 4.2 K liquid helium at one atmosphere. Therefore, for the peak fields (11 — 12 tesla) anticipated for ETF toroidal field coils, three viable bath cooling options exist:

- Nb_3Sn at 4.2 K nominal temperature.
- NbTi alloy, using He I at temperatures in the 2.5 — 3.5 K range.
- NbTi alloy, using superfluid helium (He II) at temperatures below the lambda point 2.17 K.

Despite its superior 4.2 K performance above 10 tesla, Nb_3Sn is an inherently brittle material, requiring special design and manufacturing techniques to accommodate its limited tolerance for tensile strain. Therefore, in order to insure the viability and reliability of TF-coil designs for near term machines such as ETF, General Atomic and Magnetic Corporation of America favor employment of NbTi alloys at bath temperatures below 4 K.

Specifically, a NbTiTa alloy, operating in a 3 K saturation temperature bath, subcooled to 2.5 K, has been selected for the basic design. An attractive alternative however appears to be use of the same material at 1.8 K using saturated superfluid helium (He II).

3.2.2. NbTi Alloy Selection

The NbTiTa alloy employed in this design was selected as a result of the Phase I portion of the Team One Program, completed during FY'79. Dr. David Larbalestier, *et al.*, of the Materials Science Center, University of Wisconsin, working under subcontract to GA, performed upper critical field (B_{c_2}) tests upon a large number of candidate NbTi binary, ternary and quaternary alloys with the goal of selecting one or more possessing the best

high field performance at temperatures below 4 K. Eventually a ternary alloy of NbTiTa, 32/43/25 by weight percent, was found to exhibit the most promising B_{c2} performance: specifically, 13.85 tesla at 3 K. This indicated that such material would offer acceptable design current densities at 12 tesla and practical bath temperatures (2.3 — 3 K). This study was reported upon in Refs. 3-1,3-2.

In order to verify and optimize the selected material's J_c performance, and insure its manufacturing practicality, MCA performed a series of process parameter tests upon a series of composite filamentary wire samples. J_c was determined over a range of magnetic fields and temperatures, as a function of heat treatment and cold work. No unusual manufacturing difficulties were encountered, and as anticipated, cold area reduction of 10^5 or more is desirable for J_c optimization. This work was reported upon in Ref. 3-3.

3.2.3. Performance of Selected Conductor

The MCA J_c performance data upon which this design is based is shown in Fig. 3-1. This data is based upon a total area reduction of 1.60×10^5:1 from an initial 4 in. diameter billet.

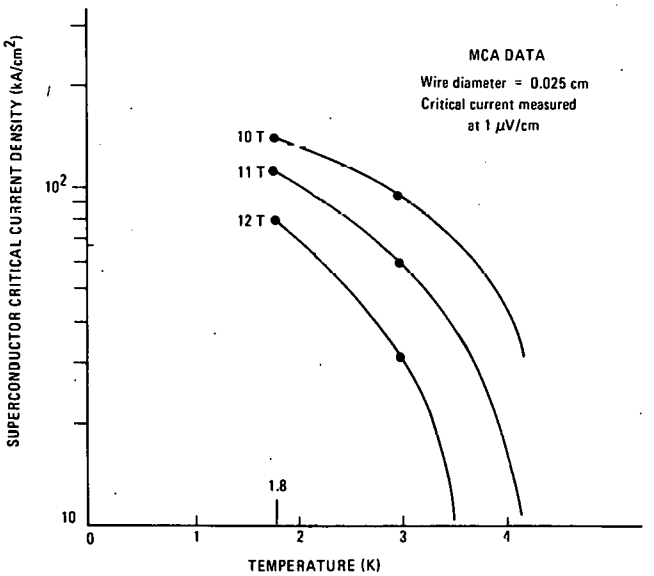

Fig. 3-1. Short sample performance of 32 Nb/43 Ti/25 Ta

3.3. COIL COOLING METHOD

3.3.1. Introduction

Bath cooling has been selected in lieu of forced flow, based upon considerations of design simplicity and operational reliability.

Forced flow cooling introduces complexities of conductor design, pumping, and parallel path manifolding which, in the opinion of GA and MCA, offset any potential benefits of improved heat transfer. In principle, forced flow cooling through simple well defined channels is well understood and is characterized by relatively high heat transfer rates (example: "hollow" monolithic conductor). However, the flow path geometries of cables or braided conductor presently under consideration for large TF-coils are torturous. Proper understanding of such geometries will require considerable analytical and experimental effort. Certainly a far greater body of practical operational experience exists for bath cooling of large superconducting coils.

The possibilities of coolant path blockage or pump failure are reliability concerns for a forced flow system. Bath cooling on the other hand is inherently reliable so long as the coils remain fully immersed in liquid.

As demonstrated in this report, even a full quench of a bath cooled coil will not damage it, provided that its design is integrated with a proper protection circuit.

3.3.2. Selected Bath Conditions

A bath saturation temperature of 3 K was selected, which corresponds to the current sharing temperature of NbTiTa superconductor at 4/3 times its design current density of 30 kA/cm^2 and 11-1/2 tesla (see Fig. 3-1 above). The corresponding operating bath pressure is 182 torr (0.24 atm, or 3.5 psia).

During normal operation, the bath is subcooled to a nominal temperature of 2.5 K. This is achieved through a heat exchanger located in the outer leg of each TF-coil.

At the subcooled temperature, the superconductor is operating at about 60% of its short sample current density.

During a local thermal disturbance (a conductor motion induced normal zone), the helium adjacent to the conductor will heat beyond the saturation temperature. The resulting vapor (bubbles) will migrate out into the bulk liquid and re-condense.

The relatively modest neutron heat load of 5 kW to the centerpost region can easily be accommodated, without bubble evolution, by natural convection within the coil.

In the event of a plasma disruption, the total field change of 0.5 tesla will generate about 7.0 MJ of eddy current heating in the ten TF-coil helium vessels (only a small amount of heat is generated in the cabled conductor). As described below in Section 5.3, this amount of heat can be absorbed by the 10 m^3 helium volume of each coil without raising its temperature above the 3 K saturation point. Thus the coil will not quench, and the bath operating temperature of 2.5 K can be restored in 4 hours by the refrigeration capacity required to absorb the neutron heating. This operating mode is shown on the helium phase diagram, Fig. 3-2.

3.3.3. Alternative Superfluid Helium Operation

A bath cooling alternative worthy of serious consideration is employment of superfluid helium.

Preliminary investigation of an ETF-like TF-coil, bath cooled with saturated He II at 1.8 K was presented in General Atomic Report GA-A15818 (Ref. 3-4).

The key characteristics of saturated superfluid helium bath cooling are as follows:

- HIGH THERMAL CONDUCTIVITY: 10^4 W/cm-K at 1.9 K and q = 0.5 W/cm^2 (this is 2×10^3 higher than annealed copper).

  As a result, almost all of the enthalpy of the entire bath volume up to the lambda point (2.17 K) is available to absorb heating from a local source.

  Heat transport takes place so rapidly that it is almost impossible to sustain an appreciable temperature gradient. Hence, all vapor evolution takes place at the liquid surface.

- HIGH HEAT TRANSFER RATE TO COOLANT: The surface heat flux from a solid depends upon several factors, but is several times that of He I. Thus the amount of stabilizer material can be significantly reduced, for a given stability criterion.

- NEAR ZERO VISCOSITY: The viscosity of He II is vanishingly small ($<10^{-11}$ poise); at least 10^6 times less than that of He I.

3.3.4. Helium Phase Diagram

Figure 3-2 is a phase diagram of helium (H_e^4). As the temperature decreases along the saturation curve past the lambda (λ) point the characteristics of helium make an abrupt and dramatic change. Above the λ-point, the substance is commonly referred to as "helium I", below it as "helium II".

Helium I exhibits properties similar to other liquids, while He II possesses unique characteristics. He II is thought of by theoriticians as being composed of two intermixed fluids; one being a normal liquid helium component while the other is "superfluid". The latter component possesses zero entropy, high heat conductivity and zero viscosity. It is often

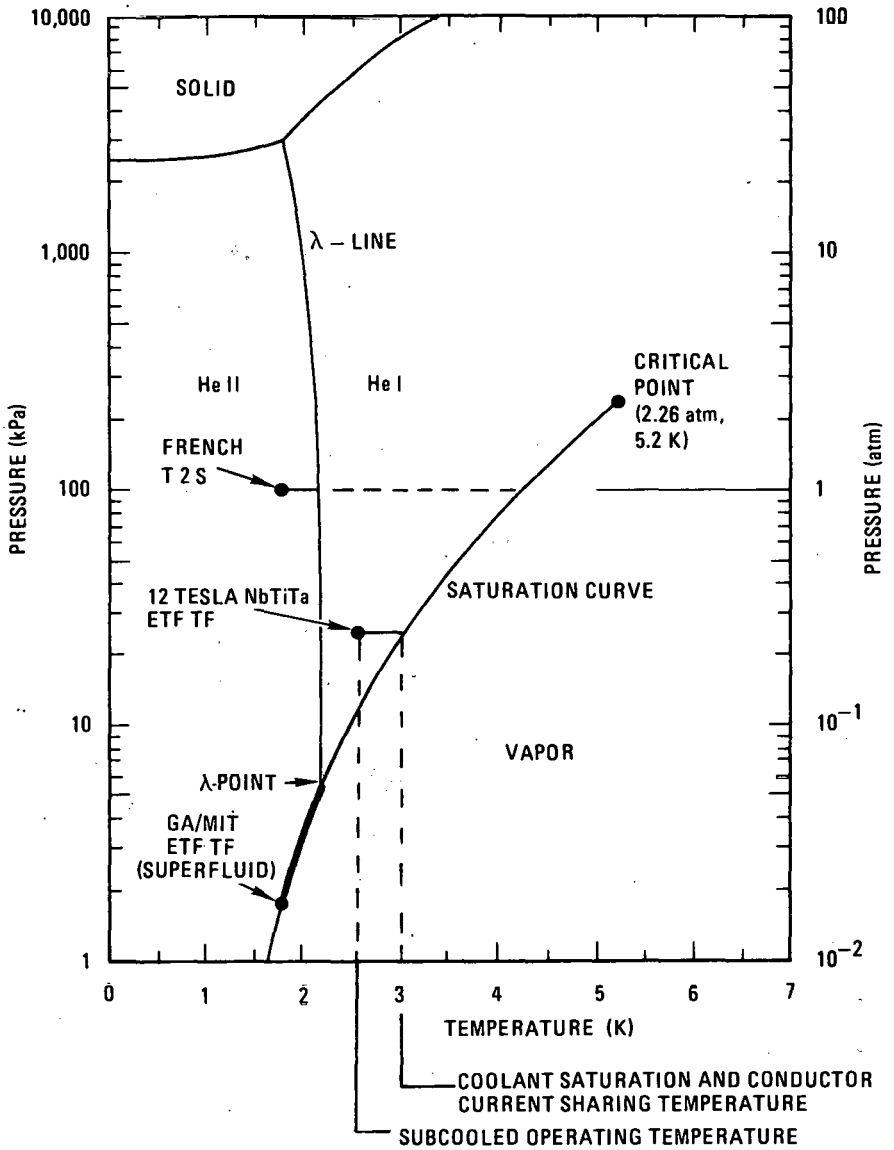

Fig. 3-2. Helium phase diagram

referred to as a "quantum fluid", its characteristics being analogous to superconducting metals in that both allow a flow of matter without friction (electron flow with zero voltage in the case of superconductors). The relative amounts of the two components of He II vary with temperature; from all normal helium at 2.17 K (λ-point) to almost all superfluid at 1.0 K. Nevertheless, by engineering convention, He II will hereinafter be referred to as superfluid helium.

Helium is also unique in that it possesses no solid/liquid/vapor triple point. It cannot be solidified, except under very high pressure (25 atmosphere at zero K).

The lambda line, which separates He I and He II is almost a constant with temperature. Thus, little temperature margin can be gained by operating at greater than saturation pressure.

Properties of helium I at 2.5 and 3 K are presented in Table 3-1.

TABLE 3-1
PROPERTIES OF HELIUM I

Property	Saturated 2.5 K	Subcooled from 3 K 2.5 K	Saturated 3 K
Temperature (K)	2.5	2.5	3
Pressure (torr)	77.49	182	182
Thermal conductivity (milliwatts/cm-k)	0.19	0.19	0.21
Viscosity (micropoise)	36.4	33.5	37.6
Enthalpy (J/g)	4.02	4.25	5.3
Latent heat of vaporization (J/g)	22.7	24.75	23.6
Specific heat (J/g-K)	2.28	2.157	2.49
Vapor-liquid density ratio	67.6	32.75	31.9
Density (g/cm^3)	0.1448	0.1455	0.1412

3.4. CONDUCTOR/SUPPORT CONFIGURATION

3.4.1. Current

The selected conductor current of 10 kA was based upon existing manufacturing capability/cost considerations, and for compatibility with the conductor to be employed in the test coil of this program (Phase III). In fact however, a TF-coil current in the 15 — 25 kA range may well prove optimal for large tokamak reactors such as ETF.

3.4.2. Conductor Configuration

A three-level uninsulated, unsoldered cable design was selected, in lieu of a monolithic or soldered cable design, for the following reasons:

1. To minimize ac losses from the poloidal field system and plasma disruptions.

2. As a conventional, modular fabrication method for producing high current conductor at reasonable cost, and with good area reduction of the composite superconducting elements.

3. For optimal cryogenic stability, by virtue of its high effective surface to area cooling characteristics.

4. For ease of coil winding by virtue of its flexibility.

Unsoldered, cabled construction would be especially attractive for Nb_3Sn conductor in order to limit both manufacturing and operational strain.

A similar three-level cabled conductor (5 kA current) is employed in the LASL/BPA 30 MJ energy storage coil presently under construction by General Atomic. The final conductor design benefited from an extensive performance and manufacturing development effort by LASL.

3.4.3. Conductor Support

Inherent in a cabled conductor design is its limited ability to support hoop and transverse bearing loads (the latter occurring in the centerpost region of a TF-coil). Therefore, in the selected design, the conductor is sandwiched between two pretensioned stainless steel strips for hoop load support, and flanked by two bearing load support strips. Austenitic stainless steel is employed for these support elements.

Conductor internal (core) support was ruled out due to the stiffness of the composite material; a serious disadvantage during coil winding. Also, additional provision must be made for support of the centerpost radial bearing loads.

A logical alternative to the multicomponent, encasing box structure selected herein is the use of a single element extruded channel (as employed by the General Electric/IGC 12 Tesla TF-Coil Design). The perceived advantages to GA of the selected structure are: ease of structural element fabrication (rolled strips versus extruded channel); flexibility during winding; and minimization of bearing stresses in the interturn insulation.

3.5. ACCOMMODATION OF PLASMA DISRUPTION INDUCED HEAT LOADS

The inevitable eddy current heating resulting from a plasma disruption must not drive the TF-coils out of the superconducting mode — that is, cause them to quench.

This is not a trivial consideration in ETF, where the widely spaced, high current equilibrium field (EF) coils are located outside of the toroidal envelope. Being loosely coupled magnetically to the disrupting plasma, they are unable to inductively absorb its energy. Thus the surrounding TF-coils experience the full field change ($\Delta B \sim 1/2$ T) resulting from the loss of plasma current.

This condition has been carefully analyzed, as described below in Subsection 5.3. The results demonstrate that the selected cabled conductor absorbs relatively little of this energy. Some 7 MJ of eddy current heat is generated within the stainless steel helium vessels; fortunately even this amount can be absorbed by the subcooled liquid helium without raising the bath to the conductor critical temperature (the point at which resistive current sharing begins).

3.6. OUT–OF–PLANE LOAD SUPPORT

A basic design decision for ETF was location of the plasma equilibrium field (EF) coils outside of the TF-coil envelope. The primary motivation for this decision is machine maintainability; to allow intact removal of the high current, superconducting outer EF-coils if required for repair, replacement or access to other major reactor components. Incidentally, this philosophy has been adopted also for INTOR and the STARFIRE commercial reactor study.

Despite its perceived overall advantage, external location of the EF-coils requires that their total current be increased by a factor of five relative to the alternative location within the TF-coil bore (but necessarily outside of the blanket and shield). External location of the EF-coils imposes two major burdens upon the TF-coil system: they cannot inductively react the energy of a plasma disruption; and they expose the outer TF-coil region to large fringing fields, which interact with the TF-coil current to generate immense out-of-plane (overturning) loads. This fringing field is a function both of the EF-coil currents, and of the fact that, for machine accessibility reasons, the EF-coils must necessarily be few in number. (A relatively uniform distribution of the EF-current around the toroidal envelope would exclude most of the poloidal field from the TF-coils.)

The magnitude of the overturning loads on each TF-coil is shown in Fig. 3-3. In the ETF Design Center concept as of June 1980, this load is resisted by cold intercoil web structures between adjacent helium vessels, except for a clear outer leg region about 8 m high. An immense vacuum tank

encloses all of the TF- and EF-coils, except for the 8 m high outermost region of each TF-coil, which is individually surrounded by its own vactank section. These features are shown in Section 4, Fig. 4-1.

Although GA has not thoroughly reviewed this support method, it does not appear adequate to resist the applied torques without the addition of intercoil bracing between the upper and lower high load regions, either in the form of diagonal struts or shear panels. Such a requirement would of course impose a serious constraint upon intercoil accessibility, although five of the ten intercoil bays could probably be left open.

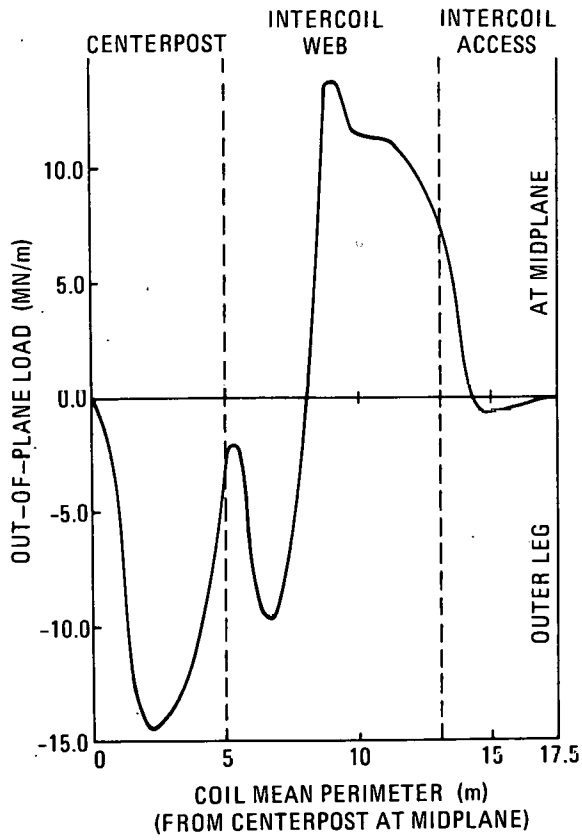

Fig. 3-3. Out-of-plane loads

3.7. VERIFICATION OF A COIL'S ABILITY TO SUSTAIN A LOSS OF LIQUID QUENCH WITHOUT DAMAGE

The ETF TF-coils must be designed to withstand a quench, or rapid transition from the superconducting to resistive state, without damage. Such an occurrence would probably never transpire during the course of a machine's lifetime, but it must be regarded as a possibility.

The primary threats to a coil under such a circumstance are excessive voltage and temperature. The engineers' task here is to design an inherently reliable coil protective (energy dump) system, and to analyze the postulated event with a reasonable degree of accuracy.

As a first principle, all of the TF-coils should be connected in series to a single power supply, in order to insure that all carry the same current. Secondly, the total dump resistance should be distributed uniformly between the coils in order to minimize the peak voltage. These intercoil dump resistors must of course be short circuited by a mechanical breaker during normal operation.

Traditionally, conductor temperature rise has been estimated on the basis of temperature versus time constant for a given copper current density, with no allowance for the changing parameters of normal region growth.

Such an approach yields grossly pessimistic results for a large coil of given substrate current density, since it fails to account for such time dependent factors as normal region size, coolant pressure, and decaying current. Therefore, a time dependent computer analysis has been developed to predict actual parameters within a quenching coil with reasonable accuracy. The results therefrom are presented in the Subsection 5.2 below.

3.8. TF–COIL AND REACTOR COSTS

3.8.1. General

For a TF-coil system with given overall dimensions, number of coils, and peak field, its cost is primarily a function of design complexity and amount and type of materials required. Beyond this, its effect on overall reactor cost depends upon several factors, including:

- Its centerpost radial thickness.
- The amount of inboard shielding required to protect the coils from excess heat load and/or radiation damage.
- The effect of its out-of-plane support structure upon machine accessibility.

3.8.2. Direct Cost Factors

One of the foundations of this concept is simplicity and, where appropriate, reliance upon techniques proven in previous large, successful superconducting magnets. For example, the method of pancake winding the coils directly into the inner wall, and against both sides of a central radial flange of the helium vessel, was used for the SLAC LASS magnet. The three-level unsoldered Rutherford cable is similar to that being employed for the BPA 30 MJ Energy Storage Coil presently under construction by General Atomic for LASL. Certainly helium bath cooling is a well proven cooling technique for large magnets.

NbTi alloy superconductor was selected for reasons of cost as well as reliability.

3.8.3. Relations to Overall Reactor Cost

3.8.3.1. Centerpost Radial Thickness – Radial thickness of the TF-coils in the centerpost region can be a major reactor cost factor if such thickness so restricts the OH-coil bore space as to force the toroidal peak field point outward beyond that set by other factors (on axis field, selected peak TF-coil field, inner shielding, etc.). It should be borne in mind however that, when necessary, the OH-coils can be embedded within the centerpost support cylinder so that the latter's thickness does not further restrict the O.D. of the OH-coils. This method was described in Volume VI, Magnetics, of the GA TNS Study, General Atomic Report GA-A15100 (October 1978) (Ref. 3-5).

In the design presented, the average centerpost coil/helium vessel current density is 1000 A/cm^2, whereas the average conductor current density is 4794 A/cm^2. This factor of 4.8 results primarily from the large amount of stainless steel strip inevitably required for hoop load support, and by the fact that cabled conductor inherently includes a substantial void fraction.

The ETF Design Center coil/helium vessel current density criterion is 1200 A/cm^2. This value could be achieved with the concept presented if the peak field were adjusted to the 10.5 tesla required (at that field the bath saturation temperature could be increased to 3.5 K).

3.8.3.2. Inboard Shielding Required – The amount of inboard shielding required to protect the TF-coil centerpost region from excessive heat load and radiation degradation is an important reactor cost factor. Reactor cost is roughly proportional to plasma radius; for ETF this amounts to at least $1M/cm.

For the ETF the inner shielding has been designed to limit the lifetime TF-coil centerpost fluence to 1×10^9 rad, equivalent to 1×10^{18} n/cm^2 (fast neutrons). The two principal considerations in this regard are mechanical degradation of the coil insulation, and electrical degradation of the copper stabilizer.

Irradiation tests at Brookhaven National Laboratory and elsewhere indicate that epoxy-fiberglass laminate (NEMA G-10) retains about 80% of its mechanical integrity up to 5×10^{9} rad.

At the design fluence, the resistivity of pure copper increases by about 8×10^{-8} Ω-cm. However, for ETF, it is anticipated that the TF-coils will be brought up to room temperature at least once during its lifetime for scheduled maintenance. Such an "anneal" will restore all but 17% of the copper's initial conductivity; hence, at the end of its operational life the radiation induced resistivity will probably not exceed about 5×10^{-8} Ω-cm. This is the basis upon which the conductor was designed.

The estimated heat flux to the coil centerpost region is 5 kW. This modest value can easily be accommodated by natural convection within the coils.

3.8.3.3. **Out–Of–Plane Support Structure** – This structure is necessarily massive in order to support the immense out-of-plane loads generated by the discrete, high current external EF-coils. The related design considerations are discussed in Subsection 3.6 above.

3.9. OPERATIONAL RELIABILITY

This is achieved through a combination of sound, straightforward design, good manufacturing practice, and comprehensive component and system testing. An effective quality assurance program is an essential element to achieve this end.

3.10. MAINTAINABILITY

At best, the removal and replacement of a TF-coil following an in-service failure would be a costly, time consuming operation. The principal difficulties here would be removal of machine components surrounding the coil, and timely manufacture of a replacement. Nevertheless, the coils should be designed for relative ease of removal from the toroidal array.

3.11. SAFETY/FAILURE MODES

3.11.1. General

Despite the most enlightened engineering, manufacturing and operational practices, certain failure modes must be considered within the realm of possibility. Two such mishaps which should be faced in the design of any superconducting magnet are a sudden inrush of air from a vacuum system rupture, and a sustained arc resulting in gross material erosion. For a properly designed and protected coil, the two failure modes of lead "crowbarring" or complete severing of the coil circuit are considered "Acts of God" — that is, situations beyond the control of engineer or operator.

Nevertheless, in all of the above cases, the TF-coil system should be designed so that, even though one or more coils may require replacement, the threat to personnel or other major reactor components is minimal.

3.11.2. Vacuum Rupture to Air

Any major vacuum rupture, such as severing of a pumping line, could result in overpressurizing of one or more helium vessels through cryocondensation of the inrushing air. Clearly, for this and other reasons, each helium vessel should include an overpressure relief valve of adequate flow capacity. A further deterrent to this threat is provided by multilayer aluminized mylar, or other insulation covering the helium vessel.

3.11.3. Sustained Arc Within Coil

The remote possibility exists that, due to a manufacturing error, a sustained low voltage (10–15 V) arc can develop within a coil during discharge. In the worst case, this can result in gross erosion of the adjacent coil structure, and differential coil currents. Although the coil would indeed be ruined, proper design of the support structure should insure that it does not damage other machine elements.

REFERENCES

3-1. D. C. Larbalestier, "Niobium-Titanium Alloy Superconductors -- Present Status and Potential for Improvement," Paper presented at the Inter-National Cryogenic Materials Conference, Madison, Wisconsin, August 21-24, 1979.

3-2. D.G. Hawksworth and D.C. Larbalestier, "Enhanced Values of B_{c2} in Nb-Ti Ternary and Quaternary Alloys," ibid.

3-3. H.R. Segal, *et al.*, "NbTi Based Conductors for use in 12 Tesla Toroidal Field Coils," Proc. of the 8th Symposium on Engineering Problems of Fusion Research, San Francisco, California, November 13-16, 1979, IEEE Pub. No. 79CH1441-5 NPS.

3-4. "ETF Toroidal Field Coil Concept Employing NbTi Alloy Superconductor and Saturated Superfluid ℓHe Bath Cooling," General Atomic Report GA-A15818 (March 1980).

3-5. "GA TNS Project, Status Report for FY-78," Vol. VI, Magnetics, General Atomic Report GA-A15100 (October 1978).

4. SELECTED DESIGN FEATURES

4.1. GENERAL

Figure 4-1 is an elevation view of ETF Design 1 showing one TF-coil. The number (ten) and overall dimensions of the Team One coil shown match those of ETF. However, its 11-1/2 tesla peak field (at 2.87 m R) corresponds to a major axis field (B_t) of 6.1 tesla.

The coil shown is 110 cm thick in the centerpost region, corresponding to its overall coil/helium vessel current density of 1000 A/cm^2. This necessitates embedding the solenoidal OH- and EF-coils within the centerpost support cylinder, as shown. This concept was employed for the superconducting OH-coils of the General Atomic TNS Reactor Study, as described in Volume VI, Magnetics, of GA TNS Project Report GA-A15100 (1978). In this scheme, each of the OH-coil segments are wound within a bobbin formed by a section of the graphite-epoxy centerpost. The TF-coils bear radially inward against the flanges of the centerpost — no radial bearing load is borne by the OH-coils. The OH-coils may be encased within individual helium vessels, or flooded through helium access ports in the centerpost sections. In the latter case, an epoxy-fiberglass helium barrier must fit tightly around the entire centerpost/OH-coil assembly (achieved through differential contraction during cooldown).

In the ETF Interim Design, cold intercoil web structures connect adjacent upper (and lower) coil regions to resist the out-of-plane loads (as shown in Fig. 4-1). An immense vacuum tank encloses all of the TF-coils, except for the 8 m high outermost region of each, which is individually enclosed. However, GA believes that several intercoil diagonal braces (or shear panels) may be required to resist opposing torsional loads of the upper and lower regions. Although not shown in Fig. 4-1, such a scheme is illustrated in Subsection 4.4.3.3 below.

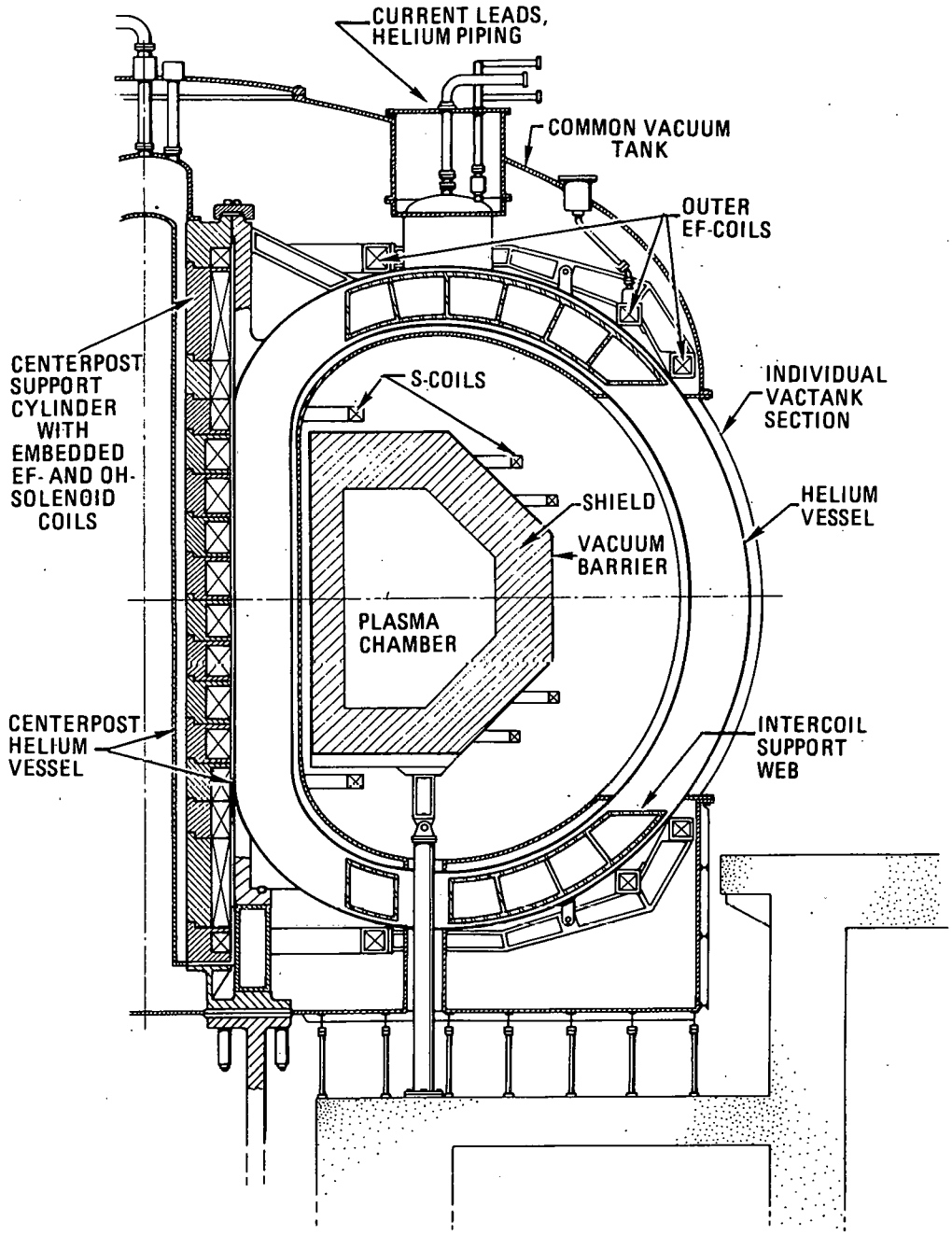

Fig. 4-1. Toroidal field coil and related reactor elements

Table 4-1 is a summary of selected TF-coil features, while Table 4-2 lists the basic calculated parameters of this system. Figure 4-2 depicts the basic dimensions of one constant tension TF-coil.

TABLE 4-1
SUMMARY OF SELECTED FEATURES

CONDUCTOR

- Superconductor Material:
  - High field regions: NbTiTa (32-43-25 wt%)
  - Low field (0 — 5 T): NbTi
- Stabilizer:
  - Material: Copper, RRR = 200:1 (minimum)
  - Maximum current density: 6 kA/cm^3 (coil protection limit)
- Operating current: 10 kA
- Geometry: Rutherford cable, unsoldered, uninsulated
- Number of field grades: Four: 0-5 T, 5-8 T, 8-10 T, 10-11-1/2 T

COOLING

- Type: Liquid helium bath
- Operating conditions:
  - Bath operating temperature: 2.5 K
  - Saturation temperature: 3.0 K
  - Bath pressure: 182 torr (0.24 atm)

COIL

- Type: Pancake (spiral) wound
  Bifurcated (two symmetric sections)
- Conductor support: Interturn stainless steel strip, plus flanking strip for bearing load support
- Ground, interturn and interlayer insulation material: Epoxy fiberglass laminate (G-10CR)

TABLE 4-1 (Continued)

HELIUM VESSEL

Material: Austenitic stainless steel

Configuration:

Coil cavity bifurcated

Trapezoidal cross section in centerpost region

Rectangular cross section in outer, curved region

Support:

Centering loads: by cold Centerpost Support cylinder: Graphite epoxy laminate

Out-of-plane loads: Cold intercoil webs, per ETF Design Center

VACUUM TANK

Material: Austenitic stainless steel

Configuration: Common vactank around coil/He vessels, except for 8 m high outermost coil region

COIL CIRCUIT

Connection: All coils in series

Design charging time: 12 hours

Protection circuit: Switch/dump resistor, parallel circuit between each coil

Dump resistor resistance: 0.25 Ω each

TABLE 4-2
ETF 12 TESLA TF-COILS — NbTi ALLOY CONCEPT
CALCULATED PARAMETERS

Total ampere turns	165×10^6
Total stored energy	40 GJ
Total inductance	800 H
Total weight of 10 coil/helium vessels	3.4×10^6 kg
Total coil height (less chimney and supports)	13.6 m
Centerpost straight section height	7.2 m
Coil/helium vessel radial thickness in centerpost region	1.10 m
Field ripple at plasma extremity	± 1.0%
Field ripple at plasma axis	± 0.10%
Mean perimeter of one coil	35 m
Average conductor current density	4794 A/cm^2
Average coil/helium vessel current density in centerpost region	1000 A/cm^2
Plasma disruption heat load to entire coil/helium vessel structure, delayed F-coil decay:	
Centerpost region (from plasma decay)	6 MJ
Outer coil region (F-coil decay)	1 MJ
Overturning moments per TF-coil, due to external F-coils:	
Outer coil region	806×10^6 Nm
Centerpost region	678×10^6 Nm

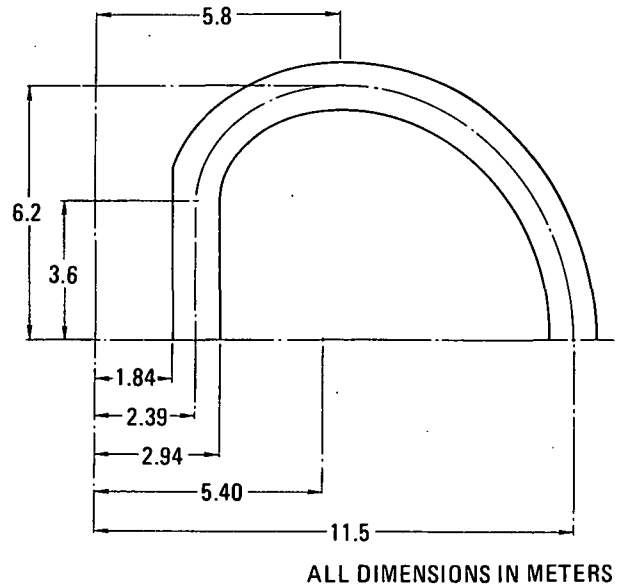

Fig. 4-2. Dimensions of coil/helium vessel, constant tension shape

4.2. CONDUCTOR

The 10 kA conductor is a three-level, unsoldered, uninsulated "Rutherford cable", whose general structure is depicted in Fig. 4-3. For ETF the final conductor consists of ten 1000 ampere cables, each of which is a six-around-one bundle of similarly configured subcables.

Four conductor grades are employed, the high and low field grades being shown in Figs. 4-4 and 4-5. Grading is based upon three centerpost region parameters: amount and type of superconductor required (as a function of magnetic field), amount of copper stabilizer required (a function of magnetoresistance, radiation degradation, cryostability and/or protection criterion limit), and required bearing load support (a function of cumulative radial bearing load).

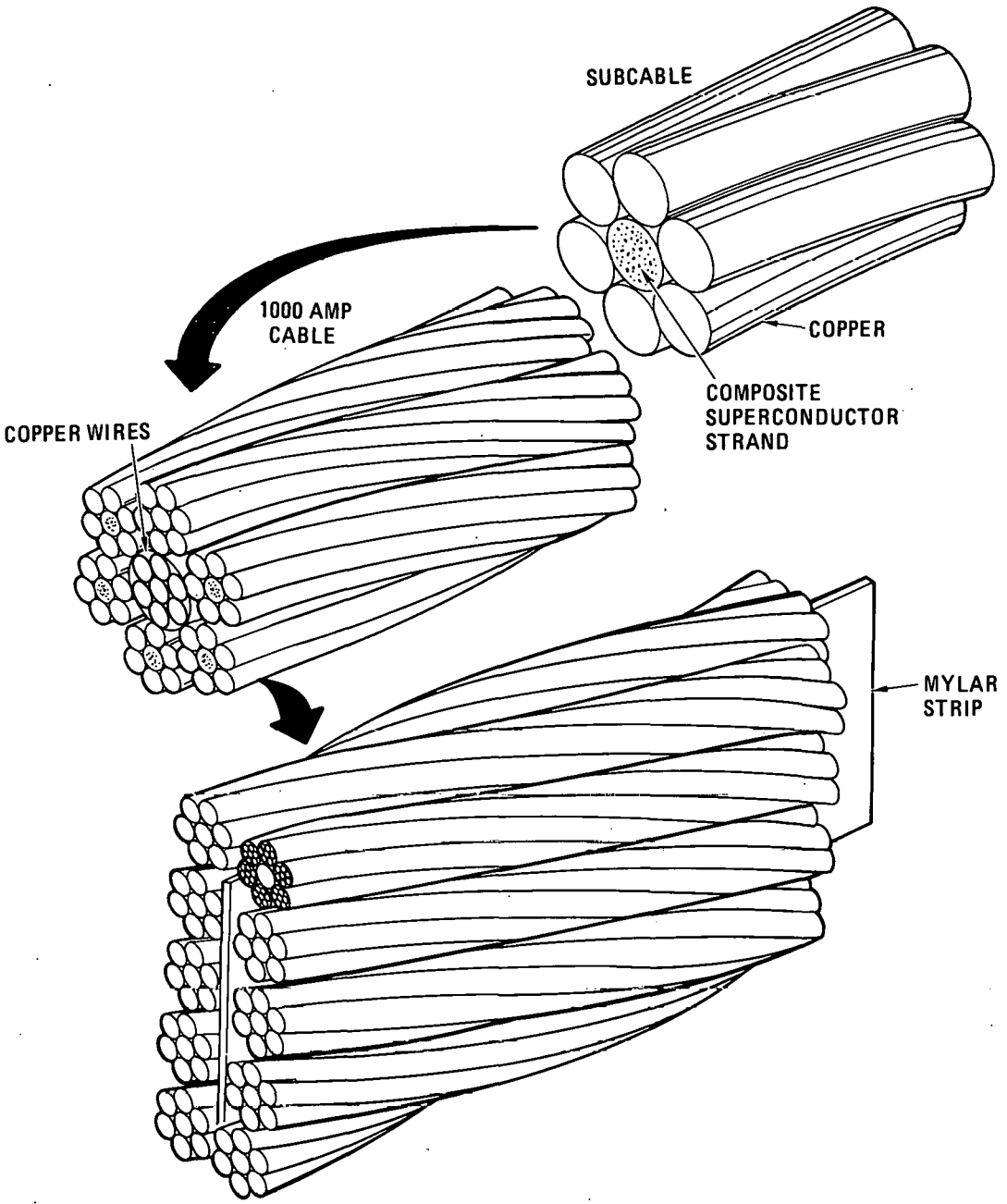

Fig. 4-3. Three-level cabled conductor low field region

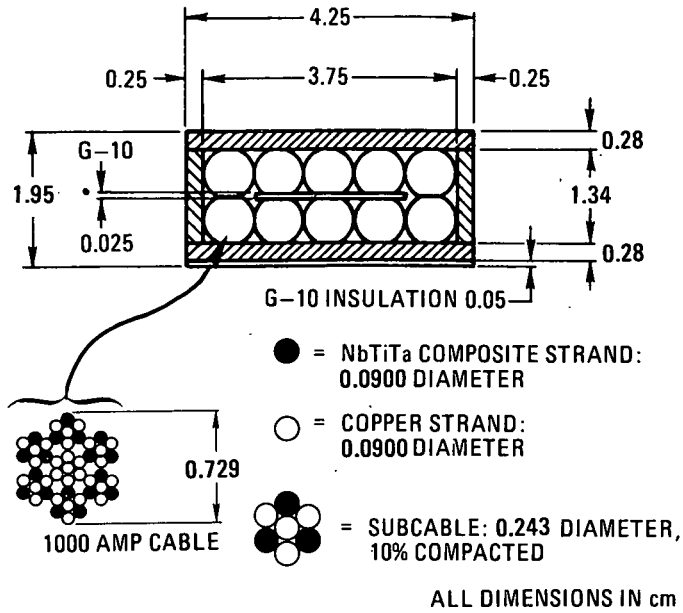

Fig. 4-4. 10 kA conductor/support module, high field region (10 — 11-1/2 tesla)

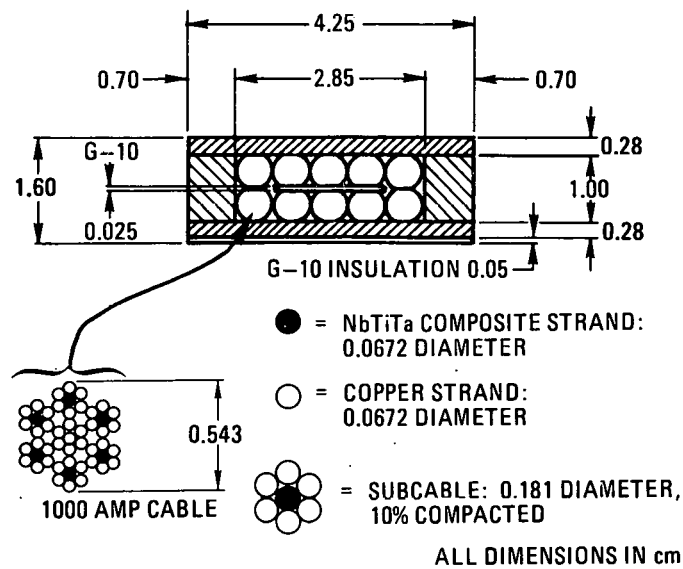

Fig. 4-5. 10 kA conductor/support module, low field region (0 — 5 tesla)

Note that in the high field region, three composite strands plus three copper strands surround one copper strand to form a subcable, while the 0–5 tesla grade has a single NbTi/Cu composite strand surrounded by six copper strands.

4.3. CONDUCTOR SUPPORT

The conductor is housed within a multi-component stainless steel strip support frame. Collectively, these support elements carry almost all of the hoop, radial bearing (centerpost) and circumferential bearing (outer region) loads generated within the coil. Allowable combined stress is 80 Kpsi (316 LN, or equivalent). The conductor, its support strips and one inter-turn insulation strip are collectively referred to as a "conductor/support module" since these components are wound simultaneously. In a pancake wound coil the coil/support module must be of constant width. Yet the stainless steel sidewall strips which flank the conductor in this design must become progressively thicker with diminishing centerpost radius, in order to bear the cumulative radial loads. Fortunately, in this and similar designs, the required conductor area, and hence width for a given number of cables, is diminishing proportionately.

This is emphasized in Fig. 4-6 which shows the high and low field conductor/support modules together. Also indicated are the helium ventilation cutouts in the sidewall support strips.

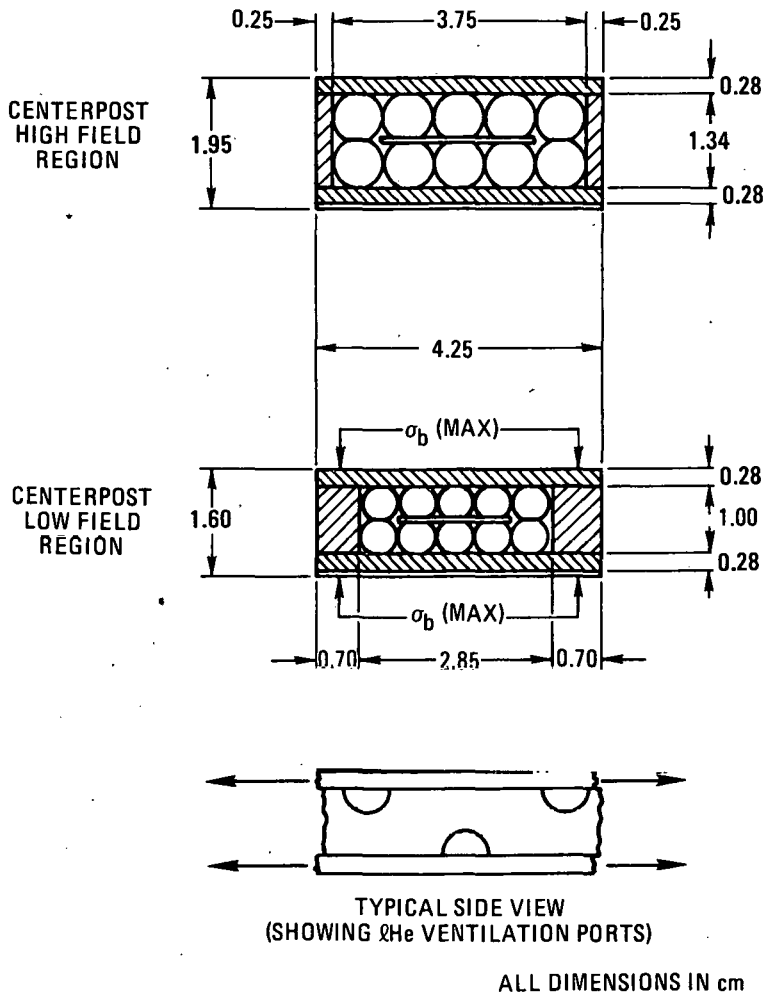

Fig. 4-6. Conductor/support modules

4.4. COIL/CRYOSTAT DESIGN

4.4.1. General

Figure 4-7 is an elevation section of one TF-coil/helium vessel, vacuum tank, centerpost support cylinder, and associated elements in the upper region. Figure 4-8 shows cross-sections of one coil/helium vessel, and related vacuum tank elements in both the centerpost, and outer region. Figure 4-9 shows the helium vessel to vactank tiebars in the outer cryostat region.

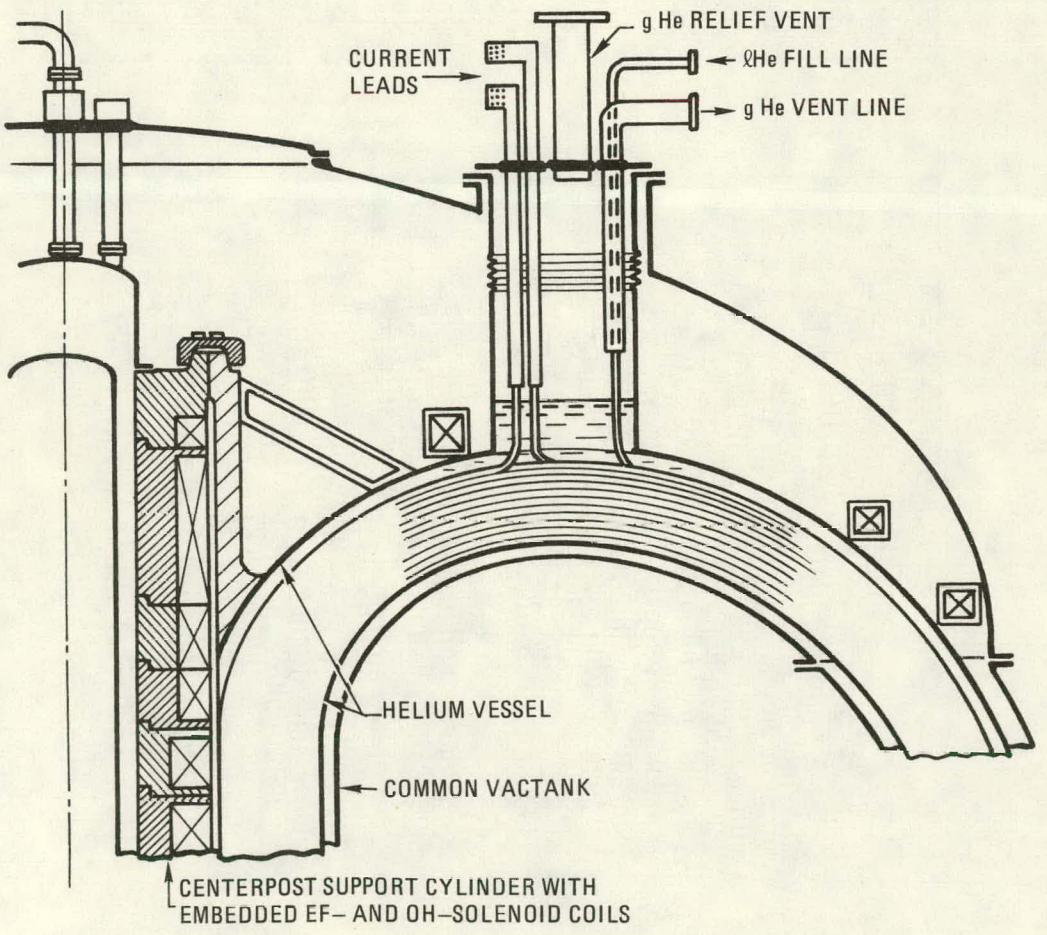

Fig. 4-7. TF-coil/cryostat and related elements section view of upper region

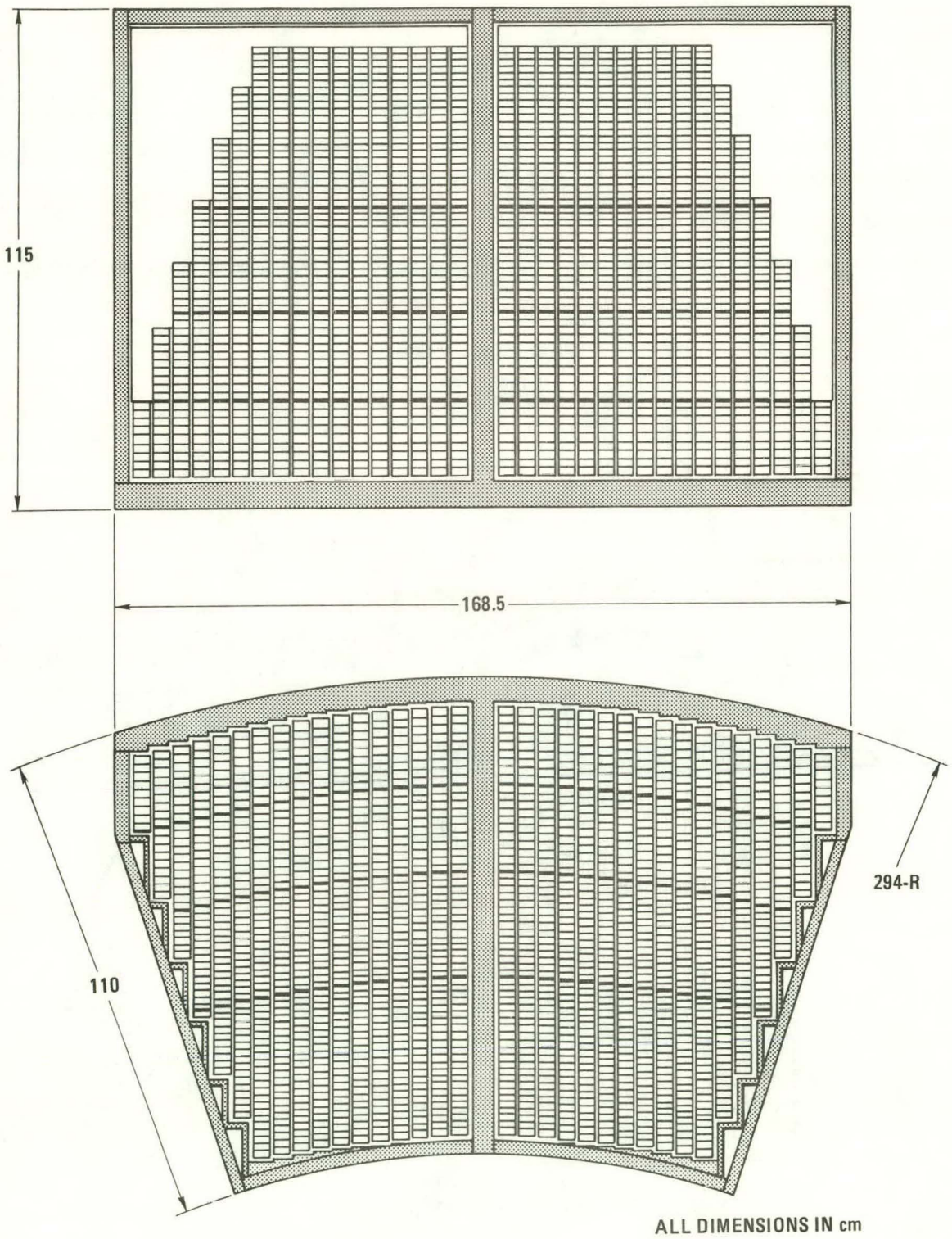

Fig. 4-8. Section through one coil in centerpost and outer region

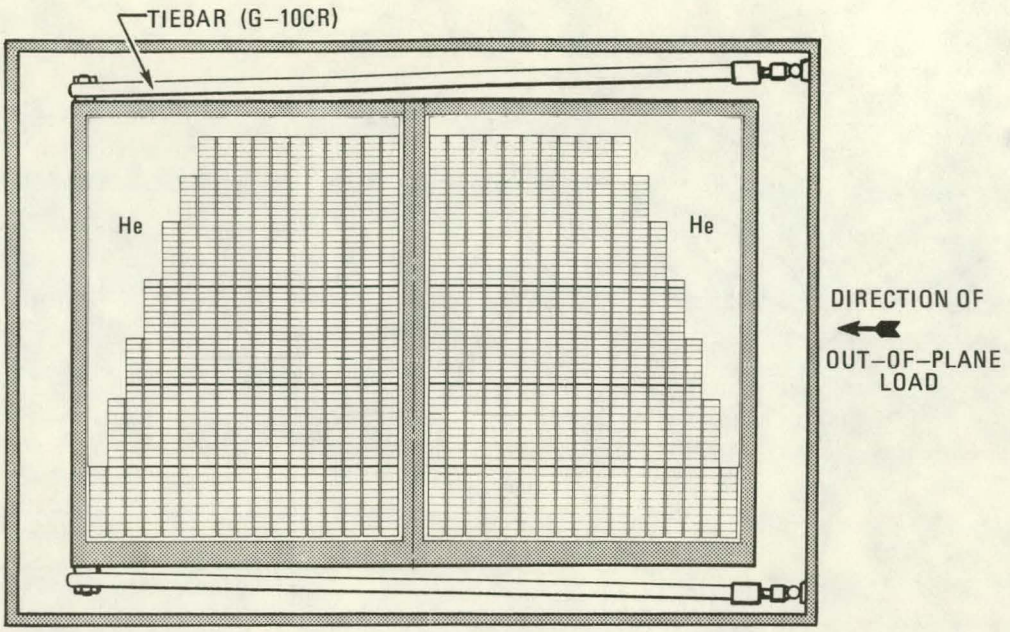

Fig. 4-9. Helium vessel to vactank tiebars in outer coil region

Each coil is independently immersed in liquid helium within its own stainless steel helium vessel. However, all 10 coil/helium vessels (plus the centerpost support cylinder, and superconducting OH- and EF-coils) share a common vacuum volume. Note that in the centerpost region, all 10 TF-coils are surrounded by a common vacuum tank; in the outermost 8 m high region each coil/helium vessel is surrounded by, and supported within its own vacuum tank leg.

Figure 4-10 is an isometric view illustrating the transition of the helium vessels from the centerpost to outer regions.

4.4.2. Coil/Helium Vessel Detail

Figure 4-11 is a cross-section of half of one coil/helium vessel in the centerpost region.

The coils are spiral wound, the 22 full height pancakes having 58 turns each. The pancakes are wound directly onto the weldment consisting of the minimum perimeter wall (the outer radius element shown in the centerpost section), and the central radial spine of the helium vessel. Thus, one-half

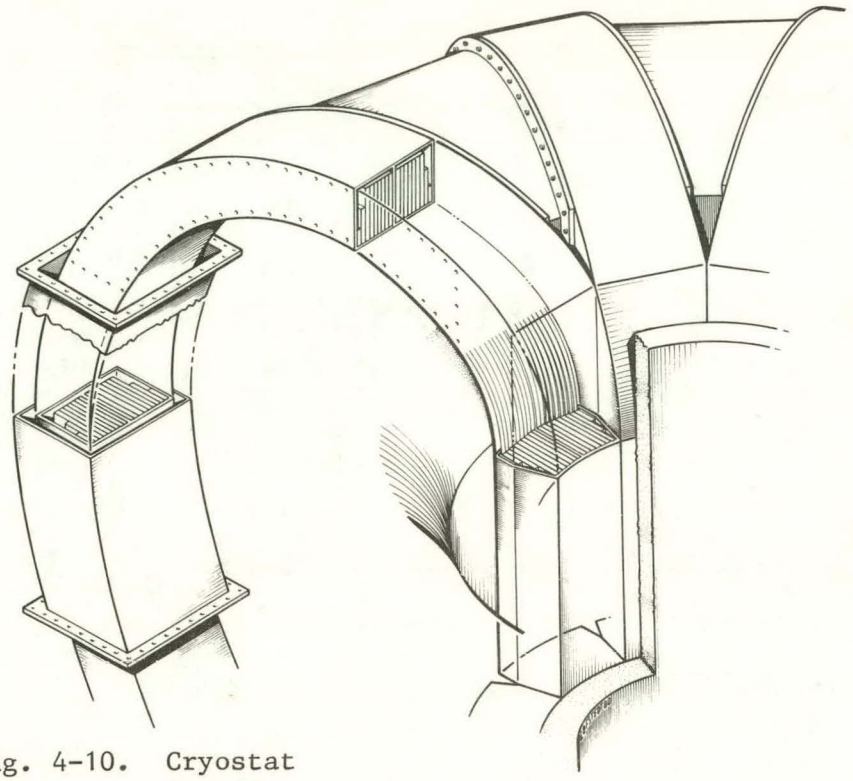

Fig. 4-10. Cryostat details

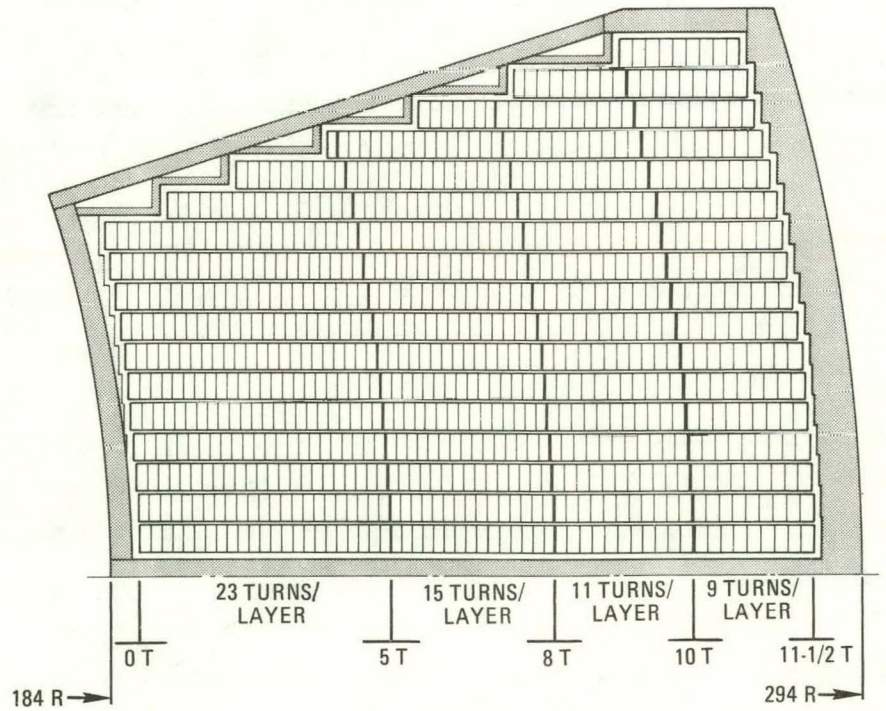

Fig. 4-11. Toroidal field coil/helium vessel half section in centerpost region

of a coil is wound and its side and outer perimeter wall elements installed. The coil/helium vessel is then inverted, and the process is repeated for the other half.

Figure 4-12 is a detail section of the coil/helium vessel, at the inner corner of the outer coil region. Shown here are detail relationships of the cabled conductor/support modules; interturn, interlayer and ground insulation, and the helium vessel. Despite its solid looking appearance in the centerpost cross section, 26% of the coil/helium vessel volume is helium. Much of this is interstitial cabled conductor space; also only about 25% of the interlayer and coil-to-ground volume is occupied by insulation material, as evidenced in Fig. 4-12.

Transverse helium migration through each conductor/support module is allowed by the twist pitch of the cabled conductor and by the cutouts (or "mouseholes") in the stainless steel side strip. Vertical helium flow is allowed by the diagonal perforation and radial groove pattern in the interlayer insulation, and by the diagonal, interrupted pattern of the coil-to-helium vessel (ground) insulation.

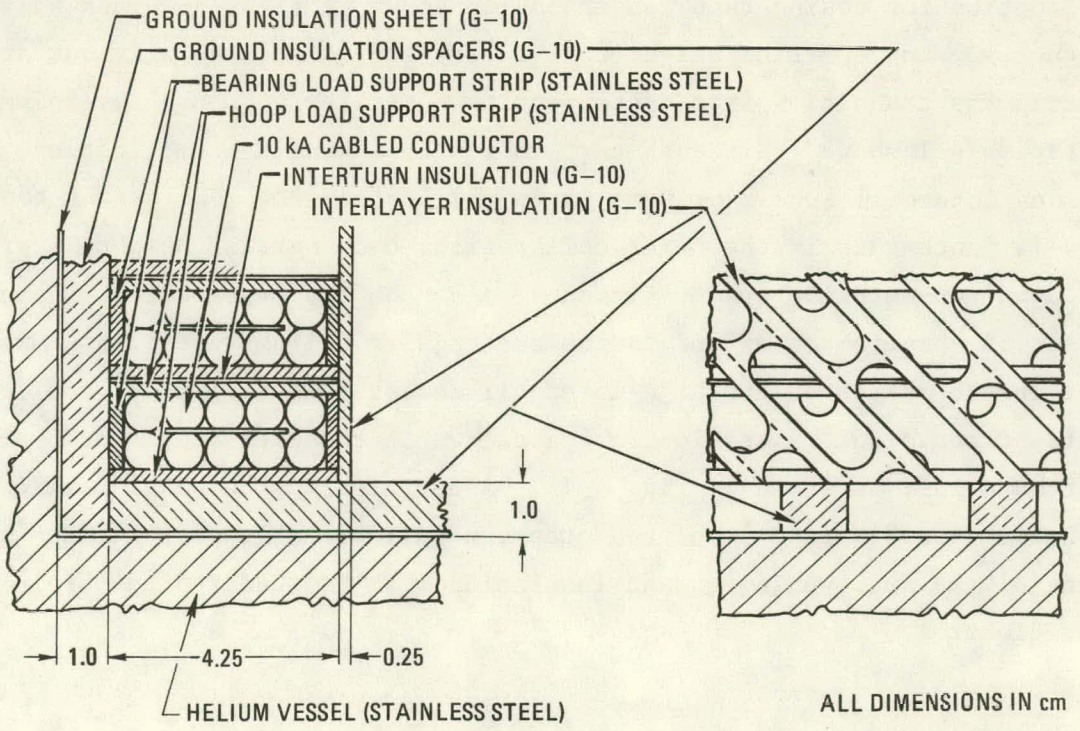

Fig. 4-12. Coil detail: High field conductor region

The coil/cryostat "chimney" region is shown in Fig. 4-7 above. Each coil has a pair of room temperature conductor leads, in order that it can be connected to adjacent coils through a dump resistor/switch circuit. These leads are cooled by helium boiloff gas. Additional boiloff gas is removed through the helium ventline, through which the ℓHe fill line counterflows. In addition, a gaseous helium relief vent is provided, set to open at 3.0 atm absolute pressure.

Although not shown in these illustrations, a subcooling heat exchanger is located within the outer, lower portion of each helium vessel. Liquid at 2.4 K is circulated through the tubes of this device in order to subcool the helium bath from its saturation temperature of 3 K to a nominal 2.5 K. Natural convection, driven by the subcooler and centerpost neutron heat load, should be sufficient to insure a reasonably uniform bath temperature.

An important design consideration for ETF is access between the outer TF-coil legs, to accommodate the neutral beams, bundle divertor, and torus sectors. In fact, this has led ETF to the adoption of a ten (vice twelve) coil array, and rectangular TF-coil cross sections. A possible coil/helium vessel option for easing this constraint is shown in Figs. 4-13 and 4-14. Here the flanking, partial height coil layers are ramped radially outward in making the transition from centerpost to outer region, thus reversing the trapezoidal shape. Although certainly a coil winding complication, the increased intercoil access of some 50 cm may justify it. (Referring to Fig. 4-14, note that in the outer coil region, each partial height layer is wound upon non-metallic spacer elements laid upon the layer below. Each such set of spacers can extend to the rectangular helium vessel inner wall, except in the outermost 8 m high intercoil access region.) Here, small spacers, trapezoidal in section, are attached to the extended interlayer spacer material, as shown in Fig. 4-13. After winding, the angled side wall helium vessel plate is placed atop the coil for closure weldment (some fitting of the intervening ground insulation will be required to obtain a proper closure).

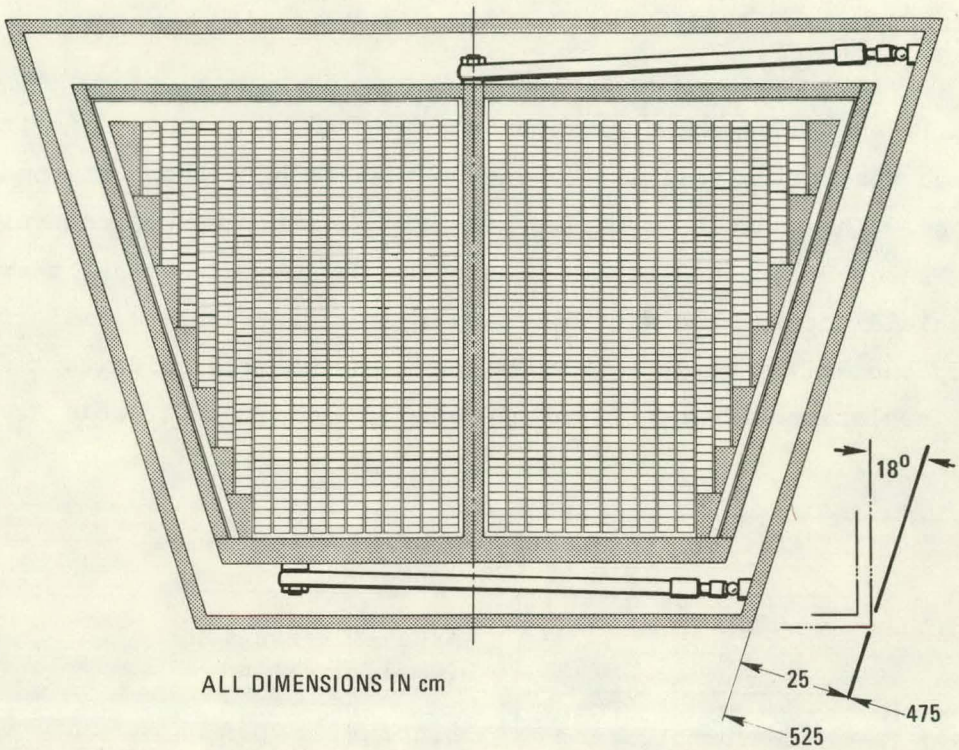

Fig. 4-13. Possible coil/helium vessel option for increasing intercoil access

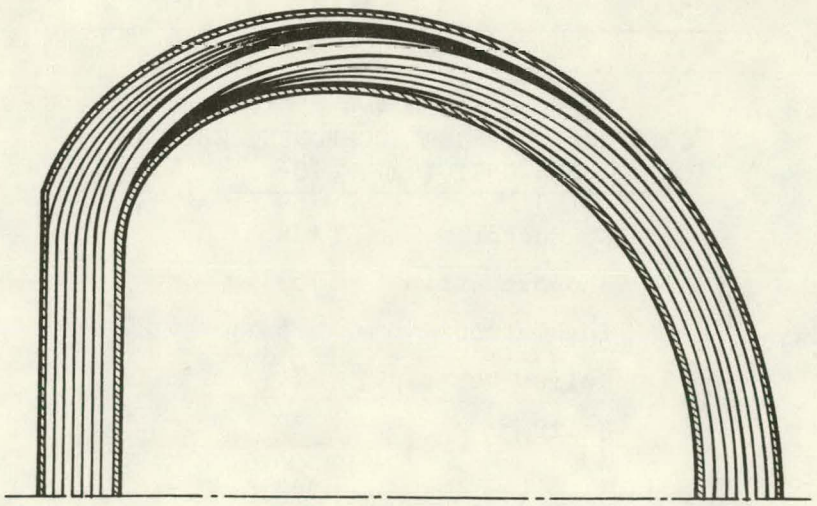

Fig. 4-14. Coil helium vessel option showing flanking layer transitions

Table 4-3 shows the coil/helium vessel component fractions in the centerpost cross section. Table 4-4 gives the component weights per coil/helium vessel.

A locally stiffened sheet aluminum thermal radiation shield is interposed between the helium vessels and vacuum tank in both the centerpost and outer regions. This shield is cooled with liquid nitrogen convectively circulating through attached tubing. Both the helium vessels and thermal radiation shield are wrapped with multilayer aluminized mylar insulation. Collectively the helium vessels, vacuum tank, thermal radiation shield, multilayer insulation and associated plumbing comprise the TF-coil cryostat.

TABLE 4-3
COIL/HELIUM VESSEL COMPONENT FRACTIONS
IN CENTERPOST REGION

	Area (cm^2)	Fraction Percent
Conductor, net	3,442	20.8
Support strip	5,447	33.0
Insulation	698	4.2
Helium vessel	2,635	16.0
Helium	4,297	26.0
	16,519	100

TABLE 4-4
COIL/HELIUM VESSEL COMPONENT WEIGHTS
PER UNIT (kg) $\times 10^3$

Conductor	108
Support strip	153
Insulation	5
Helium vessel	74
Helium	2
	342

4.4.3. Load Support

4.4.3.1. Centering Loads – In the straight, centerpost region the i dl × B (Lorentz) forces on each conductor are directed radially inward towards the machine axis. This accumulated load of about 12,400 psi average at the coil inner radius must be borne by the centerpost support cylinder (Fig. 4-1). Thus, in this region the inner radius helium vessel wall must bear against the "outer" turn of each full height coil layer (though interposed ground insulation of course). Also, the flanking partial height coil layers must bear against brackets attached to the helium vessel sidewalls (Figs. 4-8 and 4-11).

4.4.3.2. Hoop Loads – In its outer, curved portion, the coil is self-supporting against hoop loads by virtue of the conductor support strip. Therefore, the coil layers do not bear against the outer helium vessel wall except in the straight centerpost region, as seen in the upper view of Fig. 4-8 and in Fig. 4-7. This radial gap between coil and helium vessel outer wall is used as required for interlayer crossovers, stainless steel support strip terminations, and subcooling heat exchangers.

4.4.3.3. Out-Of-Plane Loads – The out-of-plane (overturning) loads as a function of perimeter are shown for one coil half in Sec. 3, Fig. 3-3. In the ETF Design Center Interim Design concept of July 1980, this load is borne entirely by the upper and lower intercoil web structure (shown in Fig. 4-15), and by bending in the outer coil legs.

In the Team One concept, the central radial web of the helium vessel bears the coil out-of-plane load, transmitting it to the inner and outer helium vessel walls (see Fig. 4-8). Although this load is immense, the outer coil region remains compacted against itself and the central flange, due to the self-generated encircling field.

In the upper, and lower, outer coil regions, the helium vessels are supported by the intercoil web structures. These elements will indeed constrain the upper (and lower) regions of all ten TF-coils to rotate about

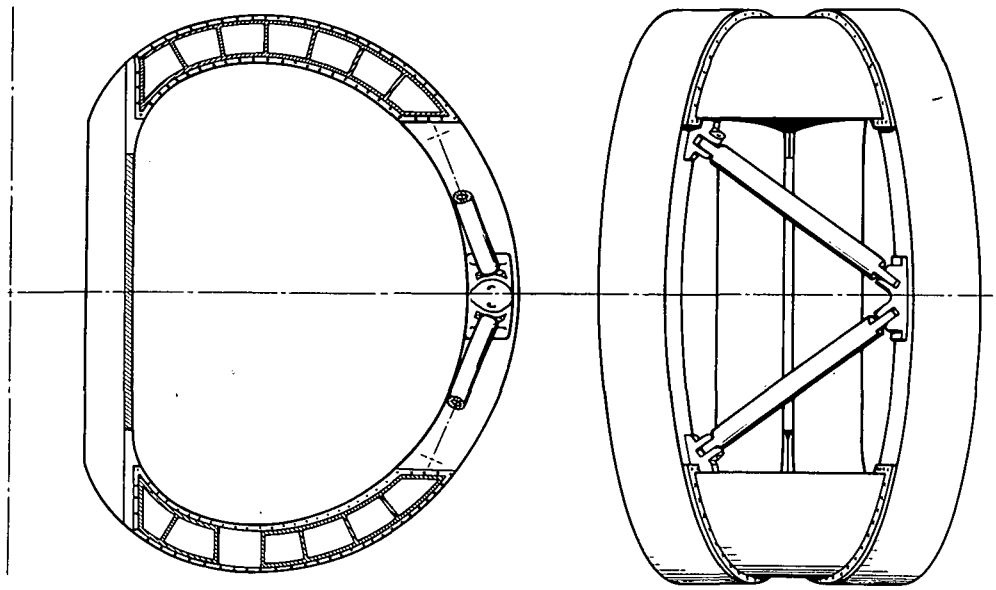

Fig. 4-15. Out-of-plane load bearing structure

the machine vertical axis as rigid "wheels", in response to the out-of-plane loads. However, it appears necessary to connect the upper and lower web supported regions with diagonal intercoil struts (or shear panels) in order to resist the torsional moment between them. Such a strut is shown diagrammatically in Fig. 4-15. (Complete analytical treatment of out-of-plane load support within ETF has not been possible, nor is it within the scope of work of the 12 tesla study.)

It is recognized that such intercoil struts (or shear panels) would interfere with machine access for the bundle divertor and neutral beams, and with torus sector removal. However, since the upper, and lower, TF-coil regions are rigidly interconnected by the web structures, diagonal struts need be included only in the five intercoil bays not required for beam and divertor access. Though necessarily at liquid helium temperature during operation, they must be demountable for torus sector removal.

In the outermost coil region, where no intercoil webs exist, the out-of-plane running load can be shared by the helium vessel and its surrounding vacuum tank element by an array of paired epoxy-fiberglass tiebars, as shown in Figs. 4-9 and 4-13.

Though details are not shown herein, it is quite feasible, and may be appropriate to resist the centerpost torsion loads by vertical shear strips located in the "V" shaped gap between the outer portions of each TF-coil straight section (see Figs. 4-8, 4-11, and 4-15).

4.4.4. Coil Winding

As shown in Fig. 4-16, each coil layer (pancake) is wound directly onto the weldment formed by the inner wall, and central radial spine of the stainless steel helium vessel. During winding, each such weldment is horizontally mounted upon a rotating winding rig, as shown in Fig. 4-17.

Hydraulic or pneumatic clamps may be required to provide radial and transverse pressure against the coil during winding, as shown in Fig. 4-16.

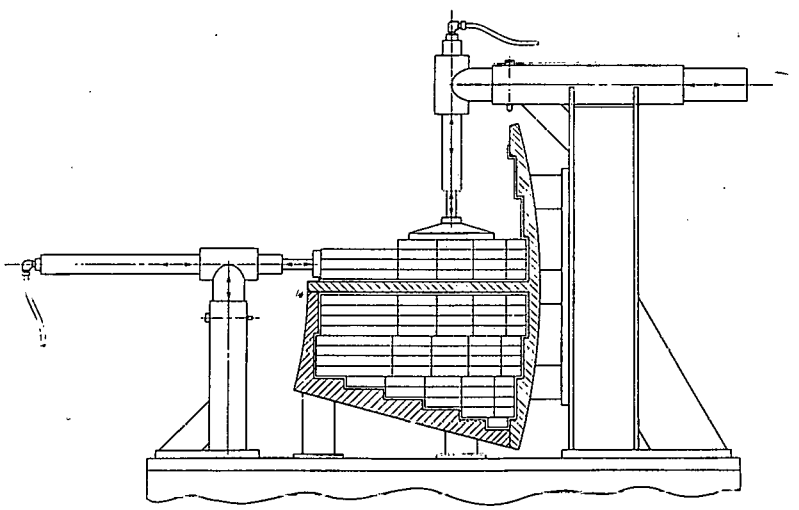

Fig. 4-16. Coil winding detail

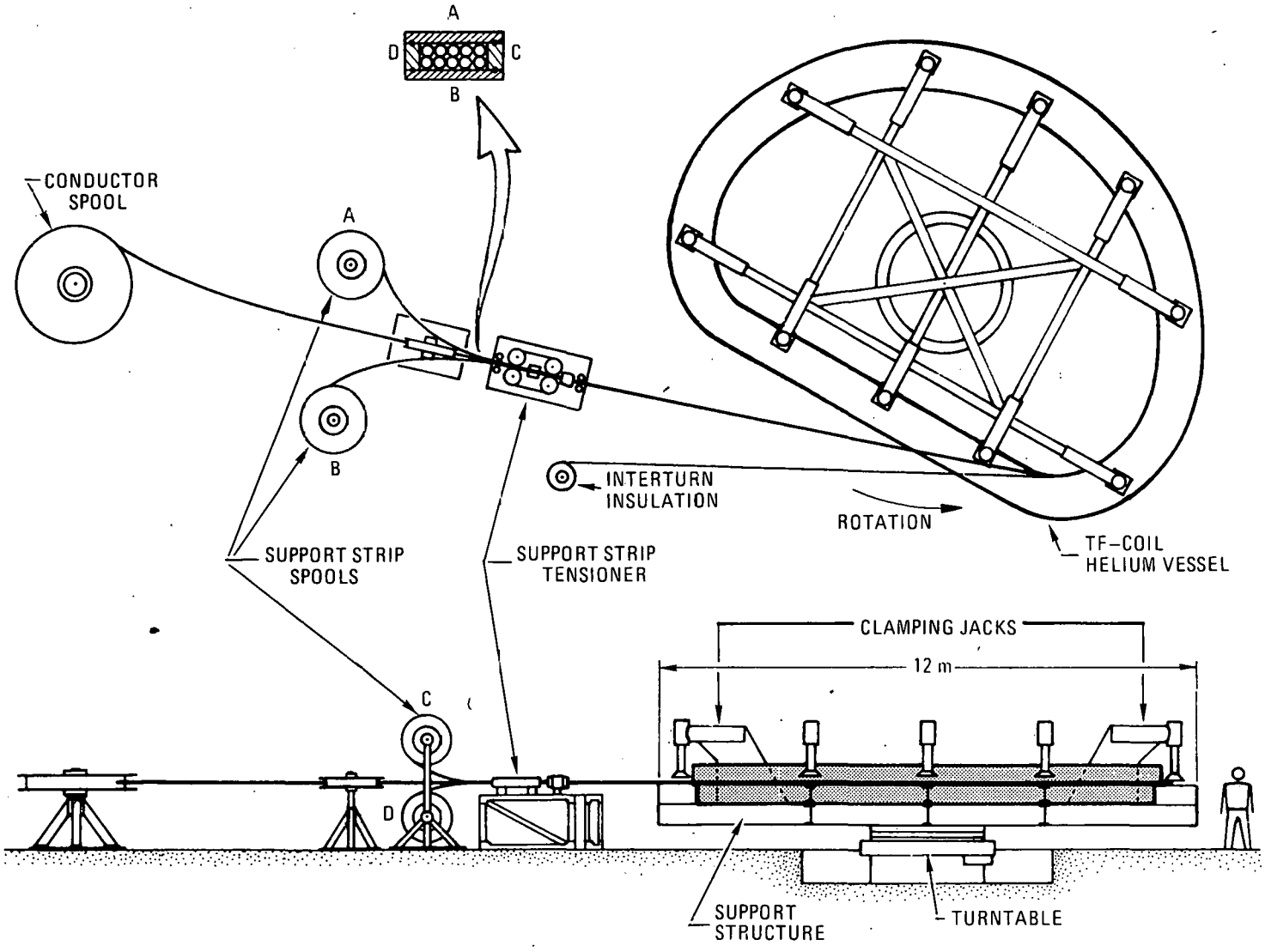

Fig. 4-17. Coil winding facility

After one-half of the coil is wound, the surrounding outer and sidewall helium vessel elements are installed. This operation may be performed with the coils still on the winding rig, since radial and vertical pressure must be applied to the plates during welding. The helium vessel structure is then inverted and the other coil half wound.

In the concept presented, the cabled conductor, four support strip elements, and interturn insulation strip must all be wound together. Further, the support strips must be wound under about 20 Kpsi pretension. As indicated in Fig. 4-17, this is accomplished by assembling the support elements around the conductor upstream of the tensioning device. (The conductor is independently given a modest pretension by "drag" on its supply spool.) The four stainless steel support strip elements are keyed together for proper alignment by length-wise grooves in the top and bottom strips, and mating ridges in the extruded sidewall strips.

Figure 4-18 shows winding, at ANL, of the superconducting pancake coils for the NAL (Fermilab) 15 foot bubble chamber magnet. The supply spools, tensioning devices, etc., are similar to those envisioned for the ETF coils. Figure 4-19 shows the arrangement used for winding the superconducting coils of the SLAC LASS magnet. The automatic (cam/solenoid operated) hydraulic pressure jacks are shown. Note that the pancakes are being wound against the inner wall, and radial flange of the helium vessel, as specified herein for the ETF coils.

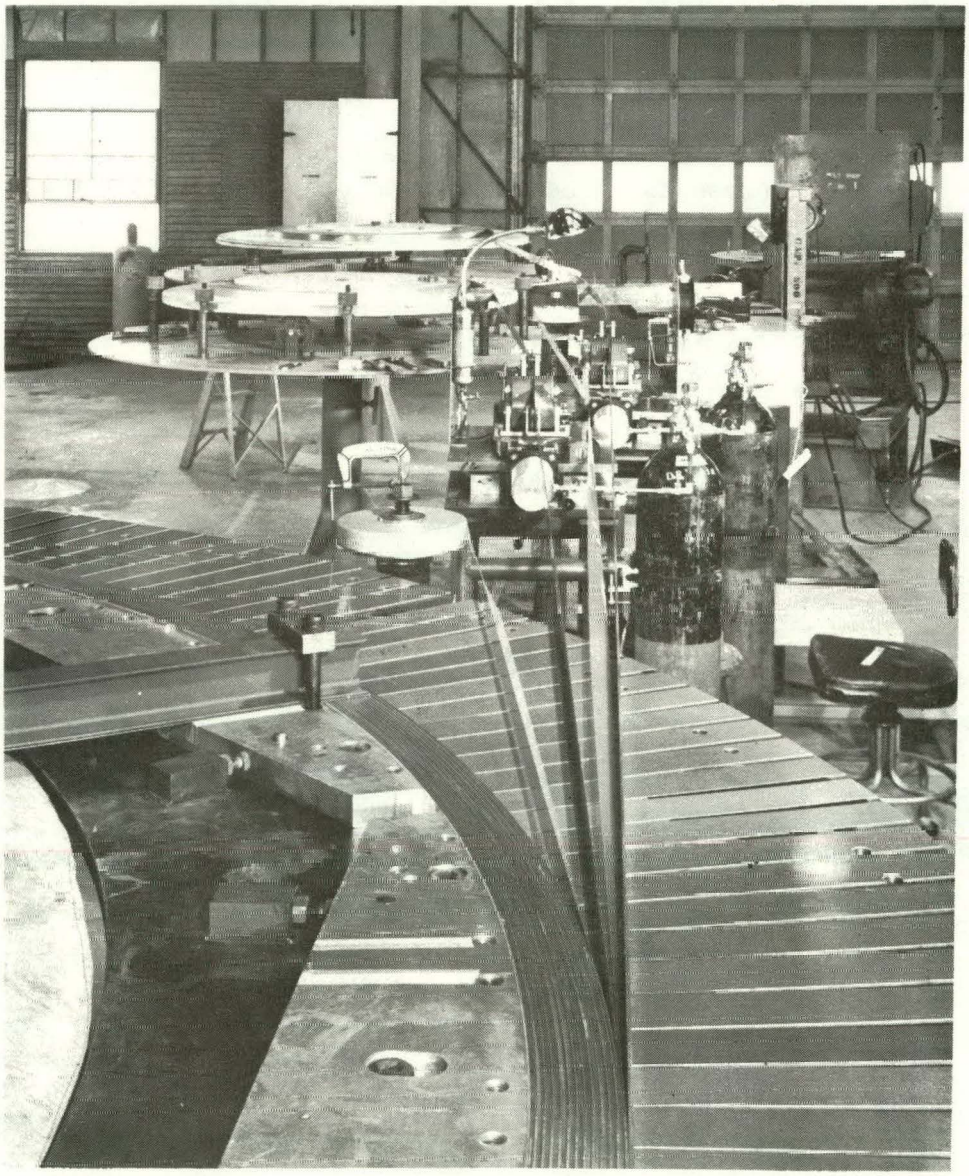

Fig. 4-18. NAL 15 ft bubble chamber
(coil winding at ANL)

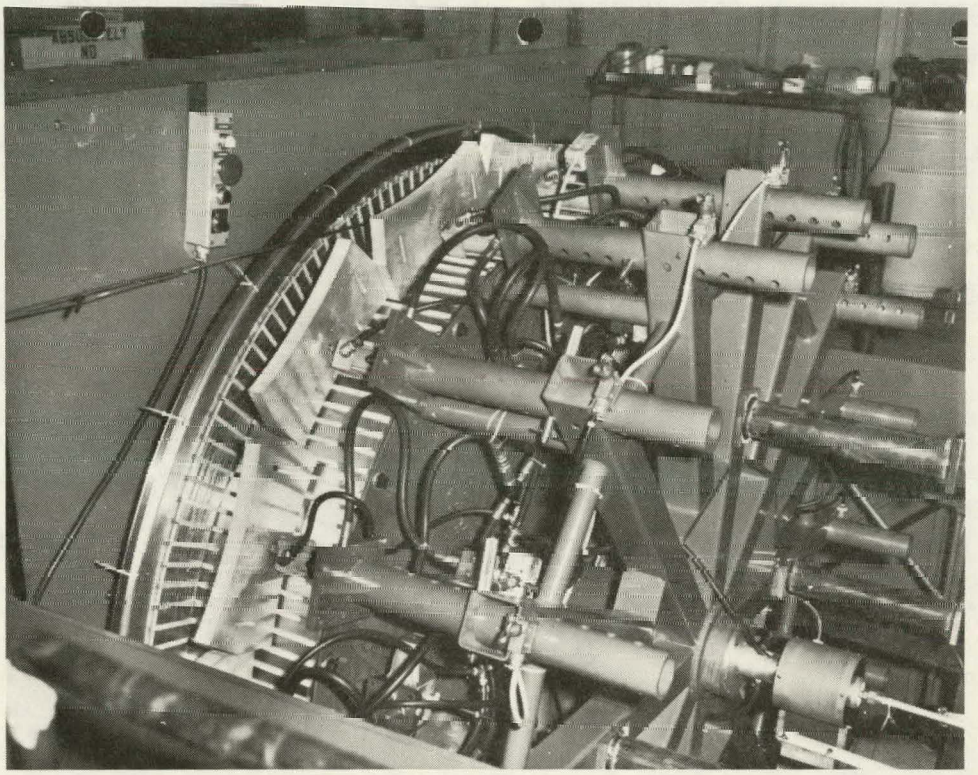

Fig. 4-19. SLAC L.A.S.S. solenoid
(coil winding apparatus)

4.4.5. Power Supply and Protection Circuit

The wiring diagram for the TF-coil power supply leads and energy dump system is shown in Fig. 4-20. The coils are charged in 12 hours during plant startup but function in a steady state mode during normal operation.

Since the stored energy of the fully charged TF-coil system is 40 GJ, coil damage would result in the event of a single coil quench if this energy were dissipated internally. To avoid this, the system is discharged rapidly by forcing the current to flow through resistors placed between the coils in the circuit and activated by mechanical switches. The 10 water cooled resistors and mechanical switches are located above the reactor, between the coil "chimneys".

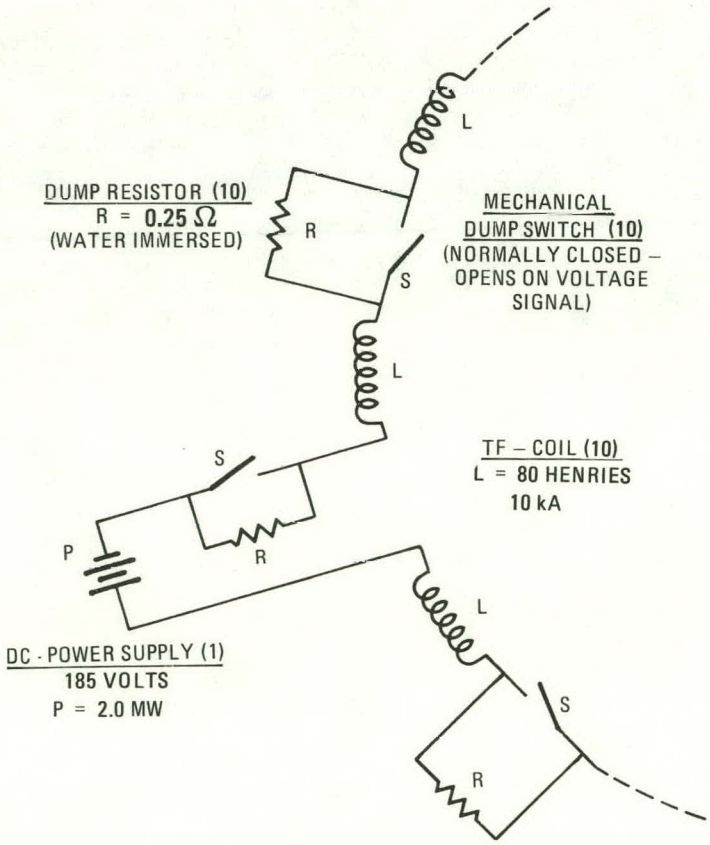

Fig. 4-20. TF-coil operating/protection circuit

During startup and normal operation, the power supply charges the coils with the dump resistors (R) bypassed by the closed switches (S). If a coil is detected to be quenching (by a voltage signal) the switches are opened, forcing the current to flow through the dump resistors.

All power and dump leads are room temperature copper conductors rated for 10,000 amps. The 20 power leads to the TF-coils are cooled by boiloff helium gas from the coil cryostats in order to minimize heat conduction to the superconductors.

Connected in series, the 10 coil toroidal arrangement has an inductance of about 800 henries. A single current-regulated power supply rated at 100 volts and 10,000 amps charges the magnet system in 12 hours. The resistance of the power leads is small and can be neglected in the charging time calculation.

The dump voltage can be limited to 2.0 kV by grounding each dump resistor at its mid-point, through a high resistance connection.

THIS PAGE

WAS INTENTIONALLY

LEFT BLANK

5. SUMMARY OF DESIGN ANALYSES

5.1. CONDUCTOR CRYOGENIC STABILITY – HIGH FIELD REGION

5.1.1. Superconductor Performance

- Critical current density of NbTiTa (32/43/25 wt%) at 11-1/2 tesla and 3 K = 40 kA/cm^2 (MCA data). See Section 3, Fig. 3-1.

- Selected operating current density = 30 kA/cm^2.

5.1.2. Stability Criterion

Conductor shall recover from a transient heat disturbance of 100 mJ/cm^3, acting over a conductor length of one meter.

- 100 mJ/cm^3 is an LCP/ETF heat input criterion. One meter length is regarded by General Atomic as a "maximum credible" motion induced disturbance for recovery.

- Equivalent radial motion under full field as represented by 100 mJ/cm^3

$$W = \vec{F} \cdot \vec{x} = (\vec{B} \times i\, d\vec{l}) \cdot \vec{x}$$

$$= 12 \text{ tesla} \times 10^4 \text{ amp} \times 1 \text{ m} \times x$$

$$x = 0.25 \text{ mm} \quad .$$

But, assume that only about half of the heat generated by conductor motion goes into the conductor itself. The remainder is absorbed by surrounding elements, so that $x' \sim 0.5$ mm.

— Equivalent conductor temperature increase:

$$\text{For copper: } \int_{o}^{25} C_p \, \Delta T = 90 \text{ mJ/cm}^3 = \Delta h$$

$\therefore$ Conductor peak temperature $\simeq$ 25 K.

5.1.3. Method of Analysis

Recovery is calculated by a computer program which includes appropriate nucleate/film boiling characteristics, current sharing, longitudinal conduction, K(t) and $C_p(t)$. For given input values of initial heat pulse, copper area, copper resistivity, and effective cooled perimeter, the program calculates whether recovery will, or will not, occur.

The resultant conditions under which recovery will just occur can be compared with the quasi-static criterion:

$$\frac{(Q \times C.P.)_{eff}}{\ell} \left(\frac{W}{cm}\right) = \frac{I^2 \rho_{cu}}{A_{cu}} \quad .$$

The following analysis input and results are based upon one 1000 amp "second level" cable at 11-1/2 tesla.

5.1.4. Input Parameters

COPPER RESISTIVITY:

$$\rho = \frac{\rho_{RT}}{RRR} + \rho_B + \rho_n = \left(\frac{171}{200} + 0.455B + 5\right) \times 10^{-8}$$

$$= 1.10 \times 10^{-7} \ \Omega\text{-cm} \quad ,$$

where 5×10^{-8} Ω-cm = fast neutron degradation, based upon one anneal cycle, and a total fluence of 1×10^9 rad. See Fig. 5-1.

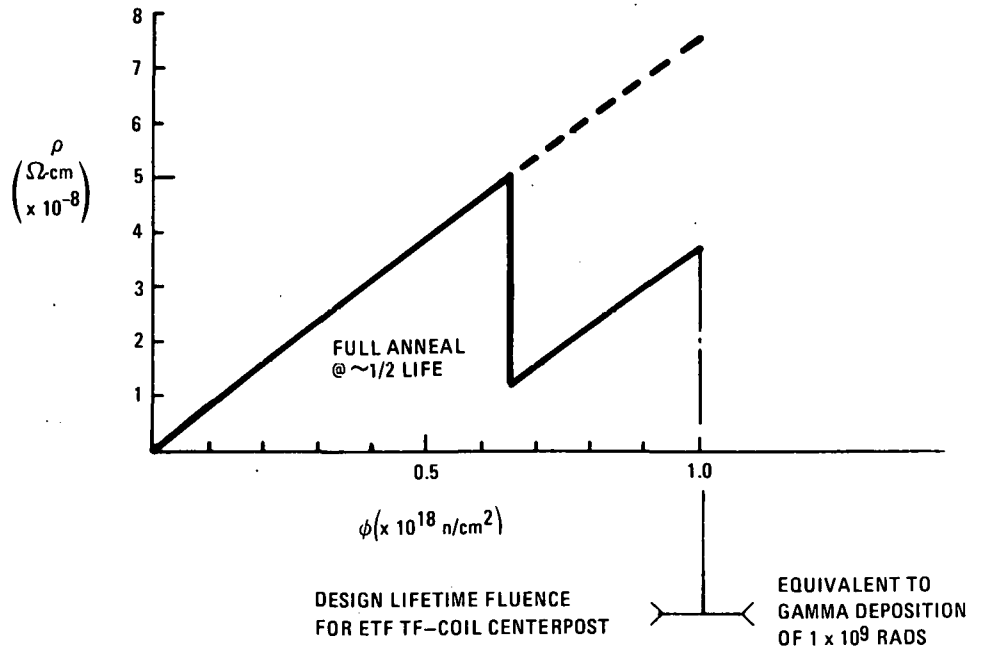

Fig. 5-1. Radiation induced resistivity increase of copper at 4.9 K, as a function of fast neutron fluence (E > 0.1 MeV) (Ref. 5-1)

ASSUMED EFFECTIVE COOLED PERIMETER:

$C.P._{eff}$ = 1/2 × "flowered" envelope of a 1000 amp cable, as shown in Fig. 5-2.

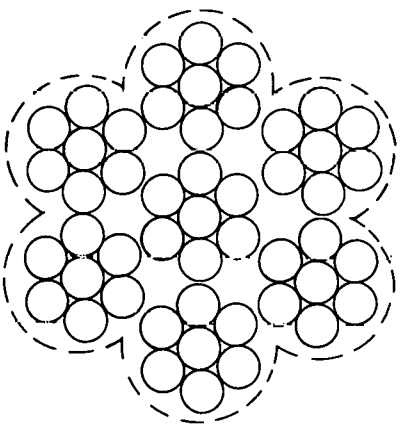

Fig. 5-2. High field conductor assumed effective cooled perimeter of one cable (= 0.50 × enclosing surface shown)

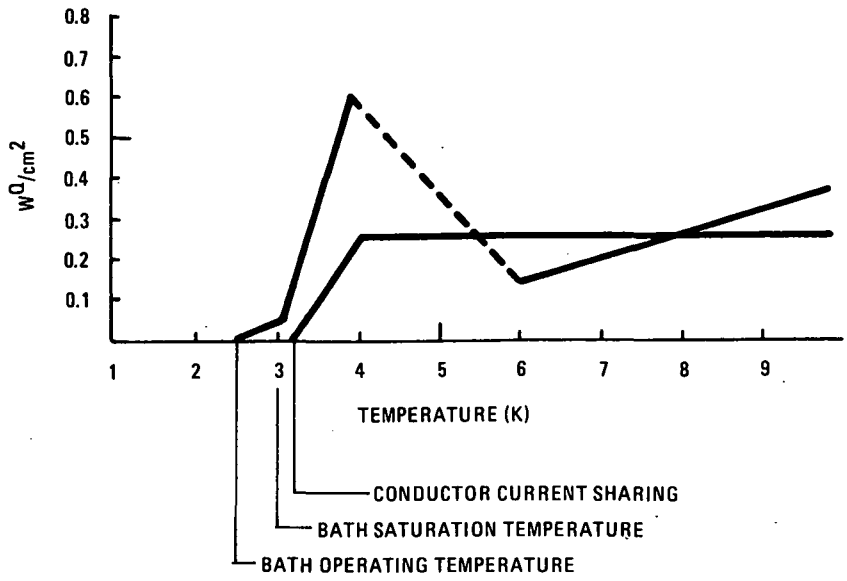

Fig. 5-3. Cooling versus heat generation in 12 T conductor normal zone

HEAT TRANSFER CHARACTERISTICS OF LIQUID HELIUM AT 3 K SATURATION TEMPERATURE:

See Fig. 5-3. Determined as described in Section 5.5 below.

HEAT INPUT:

The heat input of 100 mJ/cm^3 was translated into an initial temperature of 25 K over a length of 1 m.

5.1.5. Analysis Results

Using the above input parameters, the computer analysis indicated cold end recovery for a copper current density of 3650 A/cm^2. This corresponds to an effective maximum recovery heat transfer rate of 0.26 W/cm^2.

5.1.6. Correlation With Experimental Data

For a cabled conductor/support strip configuration as specified for this design, the product $(Q \times C.P.)_{eff}$ can only be determined with confidence by recovery tests performed using similar configurations and comparable operating parameters.

Indeed, this is one of the primary goals of the experiments to be performed upon the Team One Test Coil at the LLNL High Field Test Facility during FY'82. Also, data is being gathered with smaller but similarly configured samples at the General Atomic High Field Test Facility which will yield preliminary information and greatly assist in interpretation of the later LLNL HFTF results.

Meanwhile, as a rough guideline for this design, General Atomic drew upon recovery data performed by LASL on preliminary second-level cable for the BPA 30 MJ energy storage coil (now under construction at GA).

5.2. QUENCH PROTECTION

A magnet quench analysis for the case of a low liquid level and a normal region starting in the gas space has been performed using the GA developed code "QUENCH". This computer program accurately accounts for all the important processes in the cryostat during a magnet quench. It tracks liquid level, cryostat pressure, coil temperature, normal region dissipation, energy deposited into the helium bath, current decay, etc. The results show that the magnet will not suffer damage, provided either dump resistors are utilized or, alternatively all the liquid in the 10 cryostats is expelled at about the same time. If, however, all the energy in the TF-coil system were to be dumped into one coil it would be severely damaged by both voltage breakdown and overheating.

The computer program is basically a two-dimensional, time-dependent thermal transient code with liquid helium cooling in the region just below the liquid level. The behavior of thermal transport in the third dimension is extended out from the 2-D results since the thermal properties in the turn-to-turn direction are about the same as in the layer-to-layer direction.

The magnet is assumed uniformly anisotropic with simplified geometry consisting of an arc at the top and bottom and two straight sections. The thermal conductivity is assumed to be temperature independent. Magneto-resistivity and radiation induced resistivity are included in the total resistivity but do not change during the calculation. The heat capacities of the support structure, copper and superconducting material are integrated together. Local temperature dependent resistivities and specific heats enable the calculation of ohmic heating in the winding structure as the stored energy of the field is dissipated in the equivalent LR circuit. The compressibility of liquid helium is also accounted for. The pressure relief valve is set at 3 atm absolute.

Figure 5-4 shows the coil parameters as a function of time for a conductor with a copper current density of 6000 A/cm^2 and an average field of 5 T. It shows that peak resistive voltage over the normal region is 1.9 kV, while the peak temperature is 115 K at that time. The peak

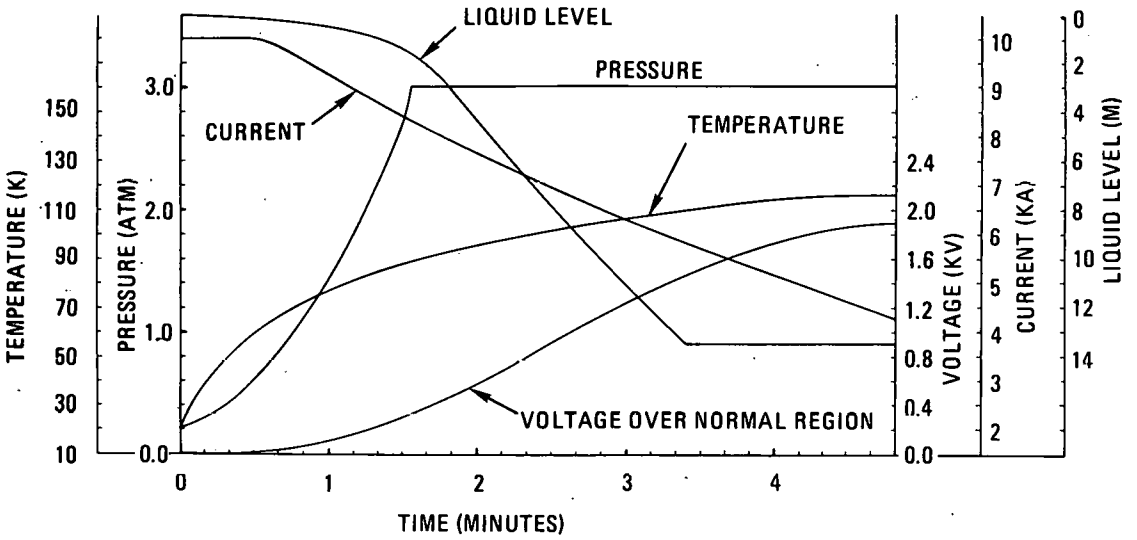

Fig. 5-4. Coil quench data

temperature rises up to 115 K in 280 seconds and would probably not exceed 120 K when the current has decayed to zero. The voltage over each 0.25 Ω dump resistor is initially 2.5 kV, being opposed by the inductive reactance of each coil as indicated in Fig. 5-5. The IR drop does not produce a large voltage in the coil because part of every turn of the coil is resistive during a quench. The IR drop of each turn is almost canceled by its $\ell\frac{di}{dt}$ rise. The net accumulated voltage relative to the ground is controlled by the dump resistor.

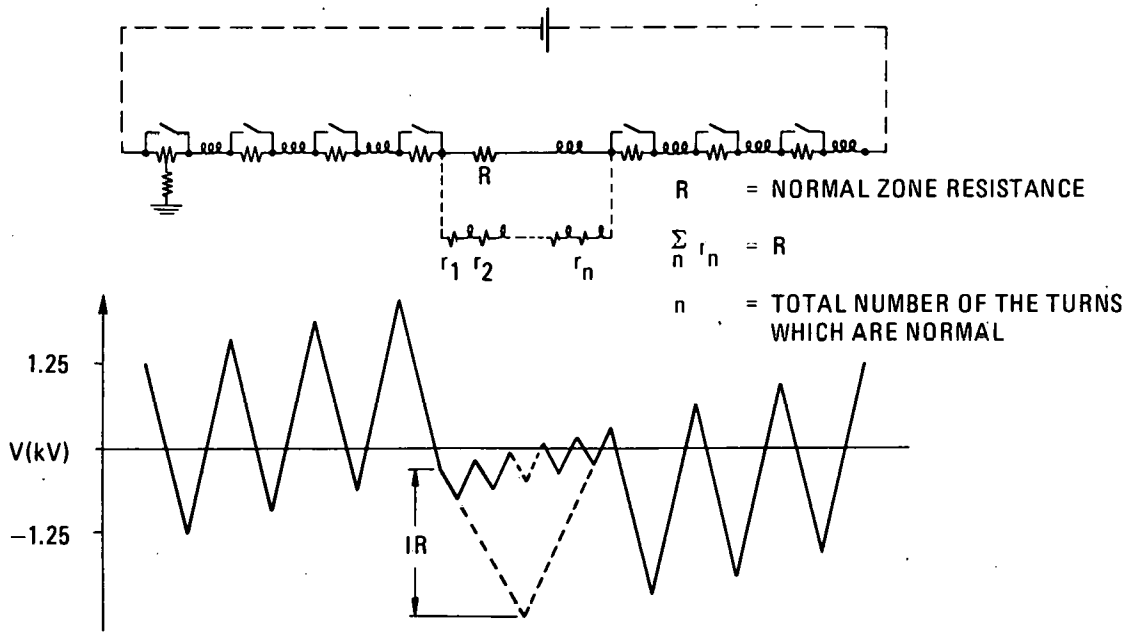

Fig. 5-5. Distributed quench voltages (shown for seven coil circuit)

5.3. DISRUPTION ANALYSES: TF–COIL HEATING DUE TO PLASMA DISRUPTION

5.3.1. Summary

The heating in the ETF TF-coil system due to plasma disruption has been estimated. Due to the utilization of low loss cabled conductor, the heating in the conductor is not the dominant heat source. On the other hand, the coil helium vessels are relatively thick and massive metallic objects, and the eddy current heating in the helium vessels represents the majority of the heat load. By controlling the poloidal coils after the disruption so that the poloidal coils are de-energized in more than one minute, the total heating can be limited to about 7.0 MJ, which will raise the helium bath temperature by 0.11 K, but otherwise should not cause other significant problems.

5.3.2. General Considerations

Due to the absence of inboard poloidal coils in ETF, when plasma disruption occurs, the centerpost region of the TF-coils will experience the fast poloidal field variation due to the abrupt disappearance of the plasma current. The plasma first wall, blanket and shield will slow down the field variation somewhat. A reasonable time duration is about 0.5 sec at the TF-coil centerpost region. The field variation in the TF-coil outer leg region will depend on the manner in which the poloidal coils are controlled after the disruption. Since the poloidal coils are relatively far away from the plasma, it should be possible to control the poloidal coils independently after the plasma disruption. A reasonable time for de-energizing the poloidal coils may be one minute.

The selected cabled conductor effectively reduces the amount of heating to reasonably low values. The coil helium vessels, on the other hand, are relatively thick, and relatively large in dimension. Each stainless steel helium vessel forms a D-shaped tubular conducting structure 40 m in circumference, about 1.55 m × 0.84 m in cross sectional dimensions, and 5 cm in wall thickness. Since the helium vessels form part of the coil structural

support against out-of-plane loads, the wall thickness must be above a certain minimum (> 5 cm). Under a pulsing poloidal field, such large scale metallic objects will develop significant amounts of eddy current heating. Since the helium vessels are kept in contact with the bath, the heat generated will eventually flow into the bath and need to be removed through the refrigeration system. Moreover, the heat input will raise the bath temperature and pressure; therefore, excessive heating may decrease the stability margin of the conductor and lead to coil quench.

It is possible to slow down the field pulse by installing flux shields around the coils. However, in the centerpost region, it is impractical to place a room temperature or liquid nitrogen temperature flux shield around each individual coil. A common flux shield for the entire centerpost can be installed, but such a flux shield may interfere with the operation of the ohmic heating coil. Furthermore, the choice of the material for the flux shield may be important in terms of strength and shielding performance. The flux shield may be utilized as part of the structure for taking the out-of-plane loads, therefore it may be necessary to use stainless steel as the flux shield material.

5.3.3. Heating in Superconductor

A three-leveled cable conductor will be utilized in the TF-coils. The conductor will be graded for a number of field regions but the pulsed field loss calculations were carried out for the 6 T field region which represents the average conditions for all the field grades. The relevant conductor parameters are listed in Table 5-1.

The distribution of poloidal field generated by the plasma current was computed using the 2-D magnetic field code EFFI. The mean square values of the perpendicular and parallel field components were then calculated. The average perpendicular field component squared $\langle B_{\perp}^2 \rangle$ is 7.93×10^{-3} T^2, and the average parallel field component squared $\langle B_{\parallel}^2 \rangle$ is 1.30×10^{-1} T^2.

TABLE 5-1
PARAMETERS RELEVANT TO LOSS ANALYSIS
FOR ETF TF-COIL CONDUCTOR

Ampere-turns per coil	15.8 MA-turns
Coil perimeter	40.0 m
Current per turn	10 kA
Conductor (6 T typical):	
Configuration	3-level, non-insulated cable, 7 × 7 × 10 strand
Strand diameter	0.0686 cm
S/C strands per cable	180
Cu strands per cable	310
Cu:Sc ratio in S/C strands	3.77:1
S/C strand twist pitch	1.5 cm
First level cable twist pitch	6 cm
Second level cable twist pitch	18 cm
Final cable twist pitch	90 cm
ρ_{Cu}	6×10^{-8} Ω-cm
ρ_{eff} ⊥ of first level cable	6×10^{-6} Ω-cm
ρ_{eff} ⊥ of second level cable	1.2×10^{-5} Ω-cm
ρ_{eff} ⊥ of final cable	2.4×10^{-5} Ω-cm

It is expected that the filament and superconducting strand coupling eddy current losses are the dominant loss components as compared to hysteresis loss. Since the coupling eddy current loss depends strongly on the transverse conductivity of the cables, the accurate estimation of the losses will require a reliable estimate of the effective transverse conductivity $\sigma_{T,eff}$.

The eddy current loss can be decomposed into the loss due to the coupling of the superconducting filaments in the strand, and the loss due to the coupling of the strands (sub-cables) in the first level cable (higher level cables).

Actual measurements of effective transverse conductivity carried out by R. Schermer at LASL on the 30 MJ coil conductor indicated that (Ref. 5-2) for the first level cable with completely uninsulated strands, the effective transverse conductivity is 10^{-2} less compared to the solder-filled cable with the same strand construction. The solder-filled cable has a conductivity comparable to Cu. Similarly, the second level cable with uninsulated strands shows another factor of two reduction in $\sigma_{T,eff}$ as compared with the solder-filled second level cable. The measurement of $\sigma_{T,eff}$ on the final cable was not carried out due to its large size. However, a conservative estimate is that going from the second level cable to the final cable $\sigma_{T,eff}$ will drop by another factor of two.

For a sinusoidal time varying field, the loss per unit volume due to the perpendicular field component is

$$P_{e,\perp}/V = 10^{-16} \times \frac{\sigma}{4} \left(\frac{H\Omega L}{2\pi}\right)^2 \left[1 + (L/2\pi\delta)^4\right]^{-1} \quad (W/cm^3) \quad , \qquad (5\text{-}1)$$

where σ = conductivity of matrix in Ω-cm

L = twist pitch of the filaments in cm

H = field amplitude in Oersteds

$\omega = 2\pi f$ with f being the frequency

δ = skin depth $= \left(2\pi\omega\sigma \times 10^{-9}\right)^{-1/2}$ (cm) ,

and the loss per unit volume due to the parallel field component is

$$P_{e,}/V = 10^{-16}\,\frac{\sigma}{2}\left(HWR_o\right)^2\left[\frac{(\ell/L)^2}{1+\left(\sqrt{2}\,\ell/\pi\delta\right)^4}+\frac{1}{16}\right](W/cm^3) \quad , \qquad (5\text{-}2)$$

where R_o = radius of the cable

ℓ = characteristic distance for field reversal.

Results of the analysis are summarized in Table 5-2. It can be seen that the total energy deposition in all 10 TF-coils per disruption is about 0.4 MJ if the plasma currents decay in 0.5 sec. It is reasonable to assume that only the plasma current decays in 0.5 seconds while the poloidal coils can be controlled to de-energize in > 1 minute.

TABLE 5-2
PULSED FIELD LOSS IN ETF TF-COIL
CONDUCTOR DUE TO PLASMA DISRUPTION

	S/C Strand	1st Level Cable	2nd Level Cable	Final Cable
Loss power per unit volume (W/cm^3)	7.44×10^{-4}	1.19×19^{-4}	5.36×10^{-4}	6.69×10^{-3}
Volume per coil (m^3)	3.78	8.83	10.3	10.3
Power per coil (W)	2.82×10^3	1.05×10^3	5.52×10^3	6.89×10^4

Total power for 10 coils = 7.83×10^5

Total energy deposition per disruption [(a)] = 3.92×10^5

[(a)] Assuming plasma current decay is 0.5 sec.

5.3.4. Heating in the Helium Vessel and Shield

If a room temperature or liquid nitrogen temperature flux shield is used to slow down the field pulse experienced by a coil helium vessel, then these two metallic structures constitute two coupled inductors, and the energy deposition on each can best be computed by a circuit simulation procedure. Variations in the external field is simulated by the introduction of the third inductor which is driven by a voltage source. Figure 5-6 is a sketch of the electrical circuit involved.

The currents in the three inductors I_i, i = 1:3 are described by the set of coupled differential equations:

$$\sum_{k=1}^{3} M_{jk} \dot{I}_k = V_j \qquad j = 1:3 \quad , \tag{5-3}$$

where V_j is the voltage drop in each inductor loop and M_{jk} are elements of the inductance matrix. The set of equations can be solved numerically given the initial conditions I_j (t = 0), and the waveform of the driving voltage $V_D(t)$.

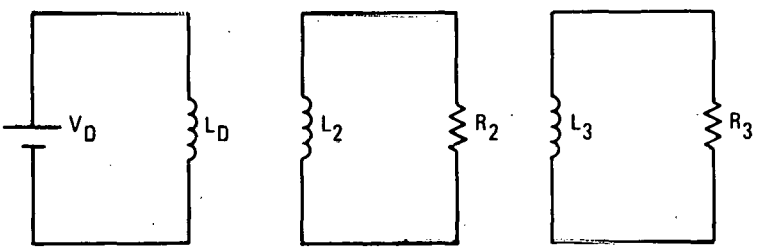

L_D = DRIVE COIL
L_2 = FLUX SHIELD
L_3 = HELIUM VESSEL

Fig. 5-6. Circuit depicting the pulsed field heating in the flux shield and the helium vessel in the outer leg region

5.3.4.1. **Outer Leg Region** – In this case, the drive coil is used to deliver the field change experienced by the TF-coil. A 10 m section of the helium vessel and vacuum vessel was simulated in the analysis. The drive coil with larger dimensions was used. The parameters of the circuit elements involved are summarized in Table 5-3.

TABLE 5-3
PARAMETERS AND RESULTS IN CALCULATING THE HEATING
ON OUTER LEG PORTION OF HELIUM VESSELS

	Shield (Vacuum Vessel)	Helium Vessel	Drive[a] Coil
Height (m)	10.0	10.0	10.0
Radius (m)	0.5	0.42	4.0
Thickness (cm)	3.0	5.0	10.0
Resistivity (μΩ)			
Stainless steel case	50.0	50.0	--
CASE 1:			
Current decay time (s)	--	--	0.5
Energy deposition[b] (MJ)			
Stainless steel case	4.22	4.15	--

[a] Used to simulate poloidal field pulse.

[b] Scaled to give total heating in all 10 TF-coil outer legs.

5.3.4.2. **Centerpost Region** – The helium vessel of each coil forms a conducting loop by itself. However, since all 12 helium vessels are closely packed into a ring in the centerpost, and a common flux shield is used to slow down the field pulse (see Fig. 5-7), the inner walls of all the helium vessels and the outer walls of them effectively forms two connected loops with equal and opposite shielding currents flowing in them (Fig. 5-7). The effective resistance of each loop is increased due to the fact that shielding currents must flow through the side walls as well. The entire system consists of four inductors, however, the condition that the inner and outer loops simulating the helium vessel inner and outer walls have equal and opposite currents can be used to eliminate one inductor from the system, and only three equations are required to fully describe the system (Fig. 5-8).

The parameters for the analysis are summarized in Table 5-4. The results are also shown in Table 5-4. Because it is not possible to further slow down the field perturbations created by the disruption of the plasma current, the 1.7 MJ of energy deposited in the helium vessels cannot be reduced very much further.

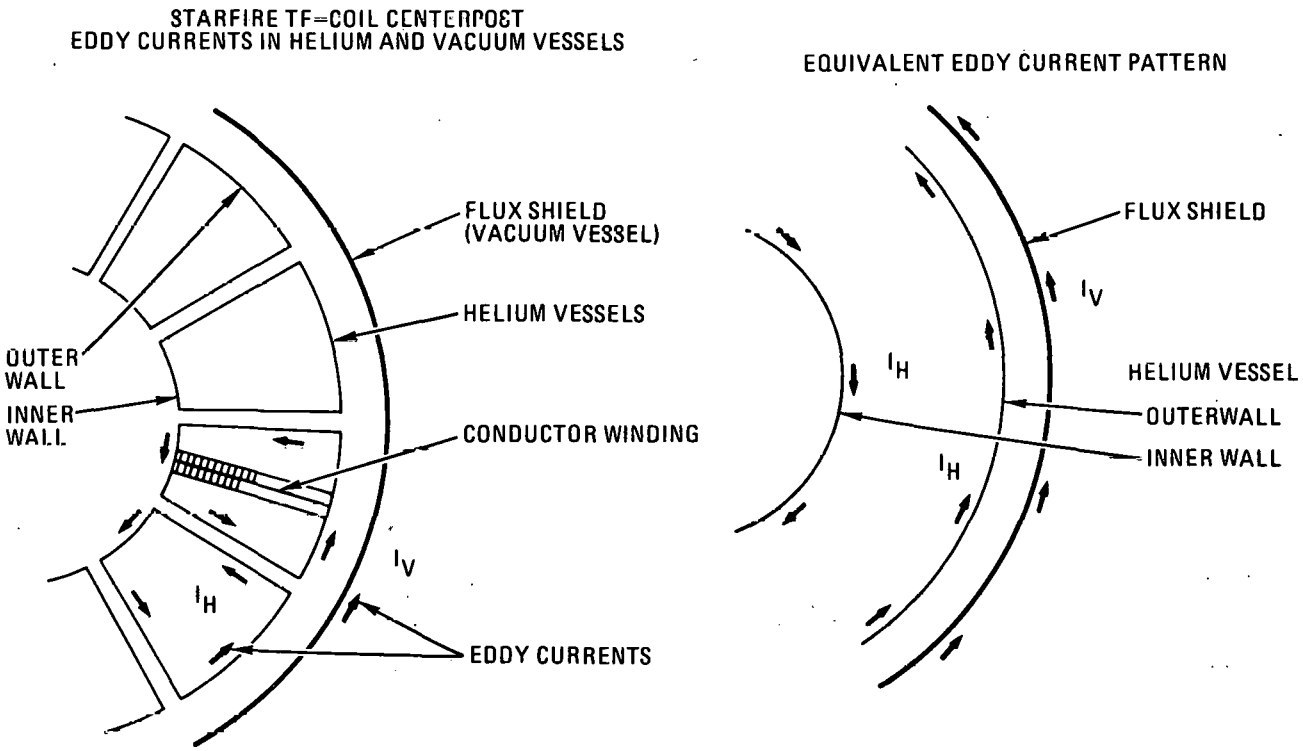

Fig. 5-7. Eddy current flow pattern in the centerpost helium vessels and flux shield

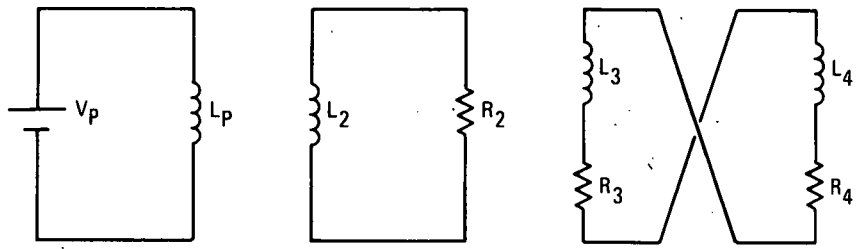

L_P = PLASMA
L_2 = FLUX SHIELD
L_3 = HELIUM VESSEL OUTER WALL
L_4 = HELIUM VESSEL INNER WALL

Fig. 5-8. Circuit depicting the pulsed field heating in the flux shield and the inner and outer walls of the helium vessel in the centerpost region

TABLE 5-4
PARAMETERS AND RESULTS IN CALCULATING THE HEATING IN THE CENTERPOST He VESSEL

	Shield (Vacuum Vessel)	Helium Vessel	Plasma
Height (m)	10.0	10.0	4.16
Radius (m)	3.00	--	5.4
Inner wall (m)	--	2.10	--
Outer wall (m)	--	2.94	--
Thickness (cm)	3.0	5.0	260.0
Resistivity (μr-cm)			
Stainless steel case	50.0	50.0	--
Current decay time (s)	--	--	0.5
Energy deposition[a] (MJ)			
Stainless steel case	13.43	1.53	--

[a] Total for 12 TF-coils.

5.3.5. Summary

The results of the pulsed field heating in the ETF TF-coils due to plasma disruption can be summarized as the following (with stainless steel vacuum vessels):

- With delayed decay (1 min) in poloidal coils:
  Total heating for 12 coils per disruption

Conductor	0.39 MJ
He vessel	6.54 MJ

5.3.6. Conclusions

- With delayed decay in poloidal coil currents, the energy deposition per disruption is about 7 MJ per coil, which can be absorbed by the helium without quenching the coil.

- Estimated bath temperature rise is 0.11 K.

5.4. HEAT TRANSFER IN SUBCOOLED ℓHe

Attempts have been made to characterize the heat transfer properties of subcooled liquid helium. A survey of experimental as well as theoretical results was conducted. The objective is to construct a numerical model for the heat transfer characteristics valid within a certain range of temperature and pressure. The numerical model will be applied to the normal zone simulation studies.

Figure 5-9 is a typical heat transfer curve for liquid helium. The meaning of the symbols are listed in Table 5-5. As seen in Fig. 5-9, there are four distinctive regions of heat transfer characteristics:

Region I. Convective region, with $T < T_{SAT}$. Since nucleate boiling does not occur until the temperature reaches the saturation temperature, natural convection is the dominant heat transfer mechanism in this region, and the typical heat flux is very low ($\lesssim 0.05$ W/cm^2).

Region II. Nucleate boiling region, with $T_{SUB} < T-T_B < T_{PNB}$. This region is characterized by the width $(T_{PNB} - T_{SUB})$, and the peak nucleate boiling flux Q_{PNB}.

Region III. Unstable region, or the transition region between nucleate boiling and film boiling, with $T_{PNB} < T - T_B < T_{MFB}$. This region is characterized by the width $(T_{MFB} - T_{PNB})$, and the minimum film boiling flux Q_{MFB}.

Region IV. Film boiling region, $T - T_B > T_{MFB}$. This region is characterized by the slope of the heat transfer curve, i.e., the heat transfer coefficient.

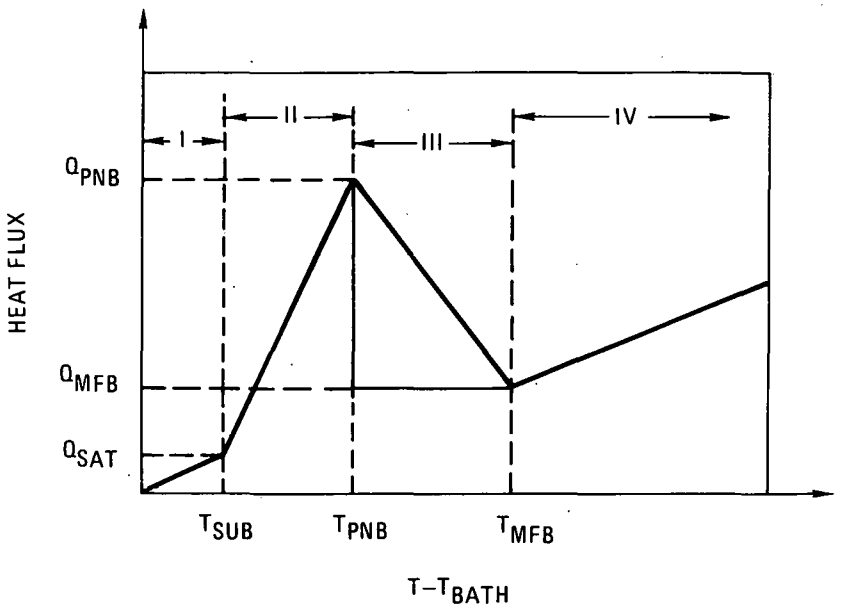

Fig. 5-9. Typical heat transfer curve for subcooled liquid helium

Experimental measurements of ℓHe heat transfer data have been carried out in numerous cases. However, most of these measurements dealt with a specific portion of the temperature range only. Very few measurements dealt with subcooled bath. Furthermore, the results of these measurements are not always in agreement.

There have been empirical or theoretical studies made on the ℓHe heat transfer characteristics. Correlations and comparisons with experimental measurements were also made. In general these correlations can provide a means of predicting the general features of the heat transfer properties in terms of the physical properties of the He liquid and vapor.

The following is an attempt to develop a model based on which the basic features of the heat transfer characteristics to a subcooled He bath can be determined approximately. The model should be able to describe the heat transfer characteristics in the temperature range $2.2\ K < T < 5\ K$, and if the amount of subcooling T_{sub} is not large ($T_{sub} \lesssim 1\ K$).

TABLE 5-5
LIST OF SYMBOLS

C_p	Specific heat
g	Gravitational acceleration, 980 cm/sec^2
h_{FB}	Heat transfer coefficient in film boiling region, W/K•cm^2
k_v	Thermal conductivity of helium vapor, in W/cm•K
L	Latent heat of liquid helium, in J/g
P	Pressure, in atm
P_c	Critical pressure of helium, (2.26 atm)
P_{SAT}	Saturation pressure of helium
Q_{MFBO}	Saturation minimum film boiling flux, W/cm^2
Q_{MFB}	Minimum film boiling flux, W/cm^2
Q_{FNDO}	Saturation peak nucleate boiling flux, W/cm^2
Q_{PUB}	Peak nucleate boiling flux, W/cm^2
Q_{SAT}	Heat flux at saturation temperature, W/cm^2
T	Surface temperature, K
T_B, T_{BATH}	Bath temperature, K
T_{MFB}	Minimum film boiling temperature, K[(a)]
T_{PNB}	Peak nucleate boiling temperature, K[(a)]
T_{SUB}	Sub-cooling temperature, K[(a)]
ρ_ℓ	Density of helium liquid, g/cm^3
ρ_v	Density of helium vapor, g/cm^3
σ	Surface tension of helium liquid, dynes/cm
μ_v	Viscosity of helium vapor, poise (gm/cm•sec)

(a) In reference to the bath temperature.

The model assumes a piecewise linear heat transfer characteristic. Then the parameters T_{SUB}, T_{PNB}, T_{MFB}, Q_{SAT}, Q_{PNB}, Q_{MFB} and h_{FB} will describe the heat transfer characteristics as shown in Fig. 5-9. Numerical fittings for some of the helium physical properties are given in Section 5.4.1.

1. REGION I, CONVECTION REGION

For a bath temperature T_B and operating pressure P_B, the sub-cooling temperature T_{SUB} is

$$T_{SUB} = T_{SAT} - T_B \qquad (K) \quad , \tag{5-4}$$

where T_{SAT} is the saturation temperature for the pressure P_B. The heat flux at T_{SAT} is

$$Q_{SAT} = 0.05\ (T - T_B) \qquad (W/cm^2) \quad . \tag{5-5}$$

2. REGION II, NUCLEATE BOILING REGION

The peak nucleate boiling temperature T_{PNB} is given by the empirical relation (Ref. 5-3)

$$T_{PNB} = 1.0 \left(1 - P_{SAT}/P_c\right) + T_{SUB} \qquad (K) \tag{5-6}$$

where P_{SAT} is the He saturation pressure for temperature T_{SAT}, and P_c is the critical pressure of He

$$P_c = 2.26 \qquad (atm) \quad . \tag{5-7}$$

The peak nucleate coiling flux Q_{PNB} is computed according to the empirical relation (Ref. 5-4)

$$Q_{PNB} = 0.22\ L\ \rho_v \left[\frac{\sigma g(\rho_\ell - \rho_v)}{\rho_v^2}\right]^{1/4} \left(1 + 1.75\ \frac{C_p\ T_{SUB}}{L}\right) \quad , \tag{5-8}$$

where L is the latent heat of LHe, ρ_v and ρ_ℓ are the densities of He vapor and liquid, respectively, σ is the surface tension, g is the gravitational acceleration, and C_p is the specific heat of He. Thus, the heat flux for $T_{SUB} < T - T_B < T_{PNB}$ is

$$Q = Q_{SAT} + \left(Q_{PNB} - Q_{SAT}\right)\left(T - T_B - T_{SUB}\right)\Big/\left(T_{PNB} - T_{SUB}\right). \quad (5\text{-}9)$$

Figure 5-10 is a plot of Q_{PNB} as a function of pressure for different amounts of subcooling, as computed according to Eq. (5-8) (Ref. 5-4). However, the value of the saturated peak nucleate boiling flux tends to be high, as can be noticed from its value at P = 1 atm.

For scaling estimations, the value of Q_{PNB} can be determined from the value of the saturation peak nucleate boiling flux Q_{PNBO} and the dependence of Q_{PNB} on ρ_ℓ, ρ_v

$$Q_{PNB} \propto \rho_v^{1/2}\left(\rho_\ell - \rho_v\right)^{1/4} \quad . \quad (5\text{-}10)$$

The value of Q_{PNBO} can be computed from the third order polynomial fitting

$$P_{PNBO} = 0.62163 + \Delta P \times \Big[1.2203 + \Delta P \times (-0.87784 + \Delta P \times 0.1054)\Big] \quad (W/cm^2) \quad , \quad (5\text{-}11)$$

where

$$\Delta P = P - 0.1 \quad (atm) \quad . \quad (5\text{-}12)$$

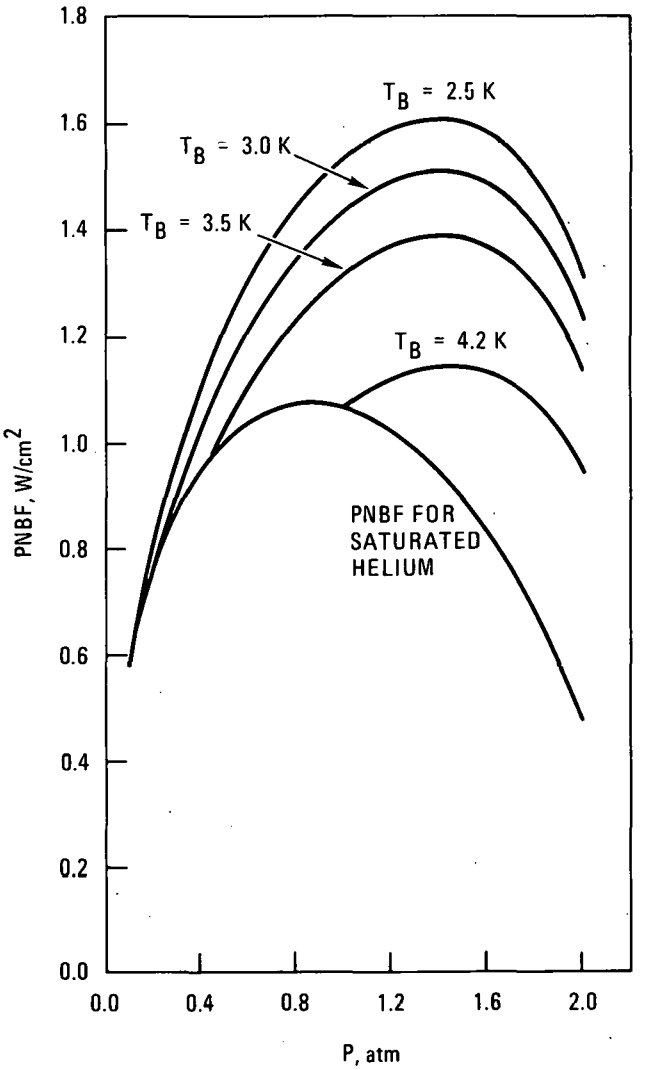

Fig. 5-10. Peak nucleate boiling flux versus pressure and subcooling

3. REGION III, UNSTABLE REGION

In the unstable region $T_{PNB} < T - T_B < T_{MFB}$, the heat transfer characteristics can be assumed to be either one of the following two forms, depending on the degree of optimism taken in the approach.

$$Q = Q_{MFB} \qquad (W/cm^2) \qquad \text{(pessimistic)} \tag{5-13}$$

$$Q = Q_{MFB} + \left(Q_{PNB} - Q_{MTB}\right)\left(T_{MFB} - T + T_B\right)\Big/\left(T_{MFB} - T_{PNB}\right) \tag{5-14}$$

$$(W/cm^2) \qquad \text{(optimistic)} \quad ,$$

The minimum film boiling temperature T_{MFB} is given by Ref. 5-3.

$$T_{MFB} = 3.25 \left(1 - P_B/P_c\right) + T_{SUB} \quad , \tag{5-15}$$

and the minimum film boiling flux Q_{MFB} is

$$Q_{MFB} = 0.14 \, L \, \rho_v \left[\frac{\sigma g (\rho_\ell - \rho_v)}{(\rho_\ell + \rho_v)^2}\right]^{1/4} \qquad (W/cm^2) \quad , \tag{5-16}$$

For scaling estimations, the value of Q_{MFB} can be obtained from the measured saturation minimum film boiling flux Q_{MFBO} and the dependence of Q_{MFB} on ρ_ℓ and ρ_v

$$Q_{MFB} \propto \rho_v \left(\rho_\ell - \rho_v\right)^{1/4} \left(\rho_\ell + \rho_v\right)^{-1/2} \quad . \tag{5-17}$$

The value of Q_{MFBO} can be computed from the polynomial fitting

$$Q_{MFBO} = 5.9478 \times 10^{-2} + \Delta P \times \Big[0.28361 + \Delta P \times \left(0.28652 \times 10^{-2} - \Delta P \times 0.72384 \times 10^{-1}\right)\Big] \qquad (W/cm^2) \tag{5-18}$$

where ΔP is given by Eq. (5-12).

Figure 5-11 is a plot of Q_{MFBO} as a function of pressure.

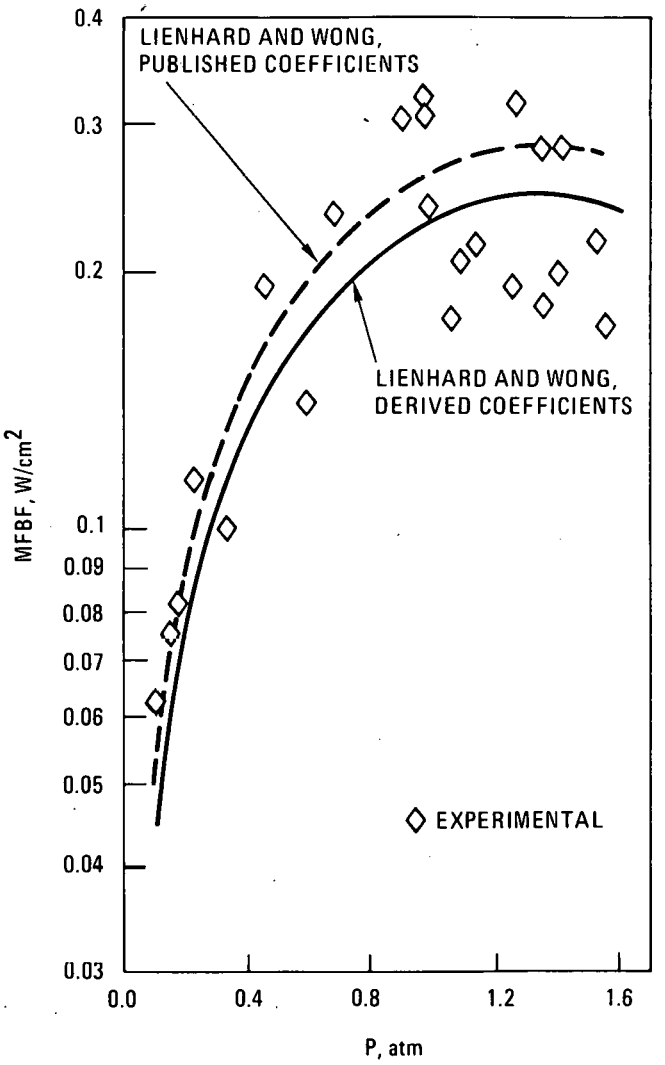

Fig. 5-11. Minimum film boiling flux versus pressure

4. REGION IV, FILM BOILING REGION

The heat flux in the film boiling region is given by $\left(T - T_B > T_{MFB}\right)$

$$Q = Q_{MFB} + h_{FB}\left(T - T_B - T_{MFB}\right) \quad (W/cm^2) \quad . \tag{5-19}$$

where h_{FB} (for a horizontal cylinder) is given by (Ref. 5-4)

$$h_{FB} = \left[\frac{\sigma}{g(\rho_\ell - \rho_v)}\right]^{-1/8}\left[\frac{\mu_v(T - T_{SAT})}{k_v^3\,\rho_v(\rho_\ell - \rho_v)\,gL'}\right]^{-1/4} \times \left\{0.37 + 0.28\left[\frac{\sigma}{gD^2\,(\rho_\ell - \rho_v)}\right]^{1/2}\right\} \quad , \tag{5-20}$$

where μ_v and k_v are the viscosity and thermal conductivity of the vapor, respectively, D is the diameter of the horizontal cylinder (or roughly the dimension of the surface), and

$$L' = \frac{\left[L + 0.34\,C_{pv}\,(T - T_{SAT})\right]^2}{L} \quad . \tag{5-21}$$

The relation (5-20) may be simplified to a form which can be used for scaling purposes

$$h_{FB} \propto \rho_v^{-1/4}\,(\rho_\ell - \rho_v)^{-3/8} \quad . \tag{5-22}$$

EXAMPLES

As examples, the following cases are presented:

1. 4.2 K bath, no subcooling, 1.0 atm pressure

The above procedure yields the following set of parameters:

$T_{SUB} = 0$ K

$T_{PNB} = 0.57$ K

$T_{MFB} = 1.84$ K

$Q_{SAT} = 0$ W/cm^2

$Q_{PNB} = 1.09$ W/cm^2

$Q_{MFB} = 0.261$ W/cm^2

$h_{FB} = 0.06$ W/K$\cdot$cm^2.

2. 2.5 K bath, 0.25 atm pressure, 0.5 K subcooling

$T_{SAT} = 3.0$ K

$T_{SUB} = 0.5$ K

$T_{PNB} = 1.4$ K

$T_{MFB} = 2.5$ K

$Q_{SAT} = 0.025$ W/cm^2

$Q_{PNB} = 0.86$ W/cm^2

$Q_{MFB} = 0.196$ W/cm^2

$h_{FB} = 0.047$ W/K$\cdot$cm^2

5.4.1. Numerical Fitting of Helium Physical Properties

Third order polynomial fits have been made to a number of physical parameters of He liquid and vapor.

1. Saturation Vapor Pressure as a Function of Temperature

If $\Delta T = T - 1.0 \quad (K) \qquad 1.0\ K \leq T \leq 5.25\ K$

Then $$P_{SAT} = \exp\left\{3.0729 + \Delta T \times \left[6.6271 + \Delta T \times \left(-1.9479 + \Delta T \times 0.21551\right)\right]\right\} \quad (N/m^2)$$

$$\left(1\ N/m^2 = 9.8756 \times 10^{-6}\ atm\right) .$$

2. Saturation Temperature as a Function of Pressure

If $$\Delta P_\ell = \ell n\ P - 2.77 \qquad \left(P \text{ in } N/m^2\right)$$

$$15.96\ N/m^2 \leq P \leq 2.264 \times 10^5 \quad N/m^2$$

Then $$T_{SAT} = 0.99835 + \Delta P_\ell \times \left[0.19837 + \Delta P_\ell \times \left(-0.035643 + 0.62852 \times 10^{-2} \times \Delta P_\ell\right)\right] . \quad (K)$$

3. Helium Saturation Liquid Density as a Function of Temperature

If $\Delta T_2 = T - 2.2 \quad (K) \qquad 2.2\ K \leq T \leq 5.1\ K$

Then $$\rho_\ell = 4.0 \times 10^{-3} \times \left\{36.688 + \Delta T_2 \times \left[-2.5274 + \Delta T_2 \times \left(1.2681 - 0.64087 \times \Delta T_2\right)\right]\right\} \quad (g/cm^3)$$

4. Helium Saturation Vapor Density as a Function of Temperature

If $\Delta T_2 = T - 2.2$ (K) $\quad 2.2\ K \leq T \leq 5.1\ K$

Then $\rho_v = 4.0 \times 10^{-3} \times \exp\left\{-1.6094 + \Delta T_2 \times \left[2.2359 + \Delta T_2 \times \left(-0.61661 + 0.10193 \times \Delta T_2\right)\right]\right\}$ (g/cm^3)

5. Latent Heat of Helium as a Function of Temperature

If $\Delta T_2 = T - 2.2$ (K) $\quad 2.2\ K \leq T \leq 5.1\ K$

Then $L = 22.491 + \Delta T_2 \times \left[4.572 \times 10^{-2} + \Delta T_2 \times \left(1.6087 - 1.038 \times \Delta T_2\right)\right]$ (J/g)

6. Helium Saturation Liquid Specific Heat as a Function of Temperature

If $\Delta T_2 = T - 2.2$ (K) $\quad 2.2\ K \leq T \leq 5.1\ K$

Then $C_{p,\ell} = 2.3055 + \Delta T_2 \times \left[1.7019 + \Delta T_2 \times \left(-2.278 + 0.96753 \times \Delta T_2\right)\right]$ (J/g, K)

7. Helium Surface Tension as a Function of Temperature

$\sigma = 9.67 \times 10^{-2} \times (5.2 - T)$ (dynes/cm) $\quad T < 5.2\ K$.

5.5. CONDUCTOR SUPPORT

5.5.1. Conductor/Support Strip Configuration

See Section 4, Figs. 4-4 and 4-5.

5.5.2. Support Strip Material and Design Stress

Stainless steel type 316LN; or 316, 25% cold worked
Minimum yield stress @ 4 K ≃ 120 Kpsi
Design maximum allowable total stress = 80 Kpsi.

5.5.3. Hoop Stress Support

Average tensile force per conductor turn:

$$T = \frac{BiR\ K}{2}, \qquad \text{where } K = \frac{1}{2}\ \ell n\ \frac{R_2}{R_1}$$

$$= \frac{12 \times 10^4 \times 2.64}{4}\ \ell n\ \frac{1.47}{2.30} = 116.4 \times 10^3\ N \quad (26{,}200\ lb)$$

High field/low bearing load region:

Thickness of top, and bottom, strip

$$= \frac{1}{2} \times \left(\frac{26.2}{80} \times 6.45\right)\ cm^2 \times \frac{1}{4.25\ cm} = 0.248 \quad .$$

Use 0.25 cm thickness for all top, and bottom support strips.

Low field/high bearing load region:

Average bearing pressure over inner radius of TF-coil centerpost

$$- \; p_i = \frac{\text{Amp-turns} \times B_{avg}}{2\pi R_i} \simeq 14 \text{ Kpsi}$$

Bearing stress in flanking support strips of low field conductor

$$\sigma_b = p_i \times \frac{\omega}{2 \omega_s \lambda_b} K$$

where ω = Top, + bottom, strip width = 4.25 cm

ω_s = Sidewall strip width = 0.70 cm

λ_b = Assumed circumferential packing factor = 0.80

K = Factor for sidewall strip helium ventilation cutouts = 1.3

σ_b = 65.0 Kpsi.

Tensile stress in support elements

Assume 50% of sidewalls are effective for tensile loads

$$\sigma_t \text{ (avg)} = 60 \text{ Kpsi}$$

Acceptable for top, and bottom strips, since

$$\sigma_t \text{ (allow)} = 80 - 0.3 \text{ (65)} = 60 \text{ Kpsi.}$$

REFERENCES

5-1. Data from 1979 U.S. INTOR report.

5-2. T.D. Thompson, *et al.*, "Losses in a Built-up Conductor for Large Pulsed Coils," paper given at the 8th Symposium on Engineering Problems of Fusion Research, San Francisco (November 1979).

5-3. V.I. Deer, *et al.*, "Nucleate and Film Pool Boiling Heat Transfer to Saturated Liquid Helium," *CRYOGENICS*, 557 (1977).

5-4. E. Ibrahim, "A Study of Pool Boiling Heat Transfer to Subcooled Liquid Helium," Ph.D Thesis, University of Wisconsin (1977).